National Oceanography Centre, Southampton
UNIVERSITY OF SOUTHAMPTON AND NATURAL ENVIRONMENT RESEARCH COUNCIL

# Development of SAR Altimetry Mode Studies and Applications over Ocean, Coastal Zones and Inland Water (SAMOSA)

## ESRIN Contract No. 20698/07/I-LG

## WP2 Technical Note

## Range Error as a Function of Significant Wave Height

**Christine Gommenginger[1], Paolo Cipollini[1] & R. Keith Raney[2]**

**[1]National Oceanography Centre, Southampton**

**[2] Johns Hopkins University Applied Physics Laboratory**

**July 2008**

## SAMOSA_WP2_NOC_v2.0



**National Oceanography Centre Southampton**
**European Way, Southampton**
**SO14 3ZH, United Kingdom**
**Tel: +44 (0)23 80596413 Fax: +44 (0)23 80596400**
Error! Unknown document property name.

## DOCUMENT SIGNATURE TABLE

| | Name | Institution | Signature | Date |
|---|---|---|---|---|
| Prepared by | C. Gommenginger | NOCS | | 19/7/2008 |
| Approved by | P. Cipollini | NOCS | | 19/7/2008 |
| Authorised by | C. Gommenginger | NOCS | | 19/7/2008 |

## DISSEMINATION

| To: | Copies | Means |
|---|---|---|
| Jérôme Benveniste | 1 | Jerome.Benveniste@esa.int |
| Salvatore Dinardo | 1 | Salvatore.Dinardo@esa.int |
| David Cotton | 1 | d.cotton@satoc.eu |
| Keith Raney | 1 | Keith.Raney@jhuapl.edu |
| Cristina Martin-Puig | 1 | cristina.martin@starlab.es |
| Ole Andersen | | oa@spacecenter.dk |
| De Montfort University, Philippa Berry | 1 | pamb@dmu.ac.uk |

## ISSUE RECORD

| Issue No. | Issue Date | Sections affected | Relevant information |
|---|---|---|---|
| 1.0 | 26/05/08 | - | Draft |
| 2.0 | 19/7/2008 | All | Implemented changes following discussions in Progress Meeting #3 (Starlab, 19 June 2008), including:<br>• Moved RV1 results to Annex 1<br>• Removed reference to SAR processing in RDSAR<br>• Added text contribution by Keith Raney in main body and Annex 2 |

# TABLE OF CONTENTS

# 1. PURPOSE OF THIS DOCUMENT

This Technical Note represents the deliverable for WP2.4 “Range Error as a Function of Significant Wave Height” of the contract ESRIN 20698/07/I-LG “Development of SAR Altimetry Mode Studies and Applications over Ocean, Coastal Zones and Inland Water (SAMOSA)”.

The objective of WP2 is to perform a scientific study of the gain in performance of the CryoSat SAR altimeter over ocean compared to conventional pulse-limited altimeters. The study aims to provide an independent assessment of the expected improvement in range retrieval with Delay-Doppler Altimetry (DDA) compared to pulse-limited altimetry for different values of Significant Wave Height (SWH). Earlier investigations by Jensen & Raney (1998; see Figure 1 report an improvement by a factor of 2.

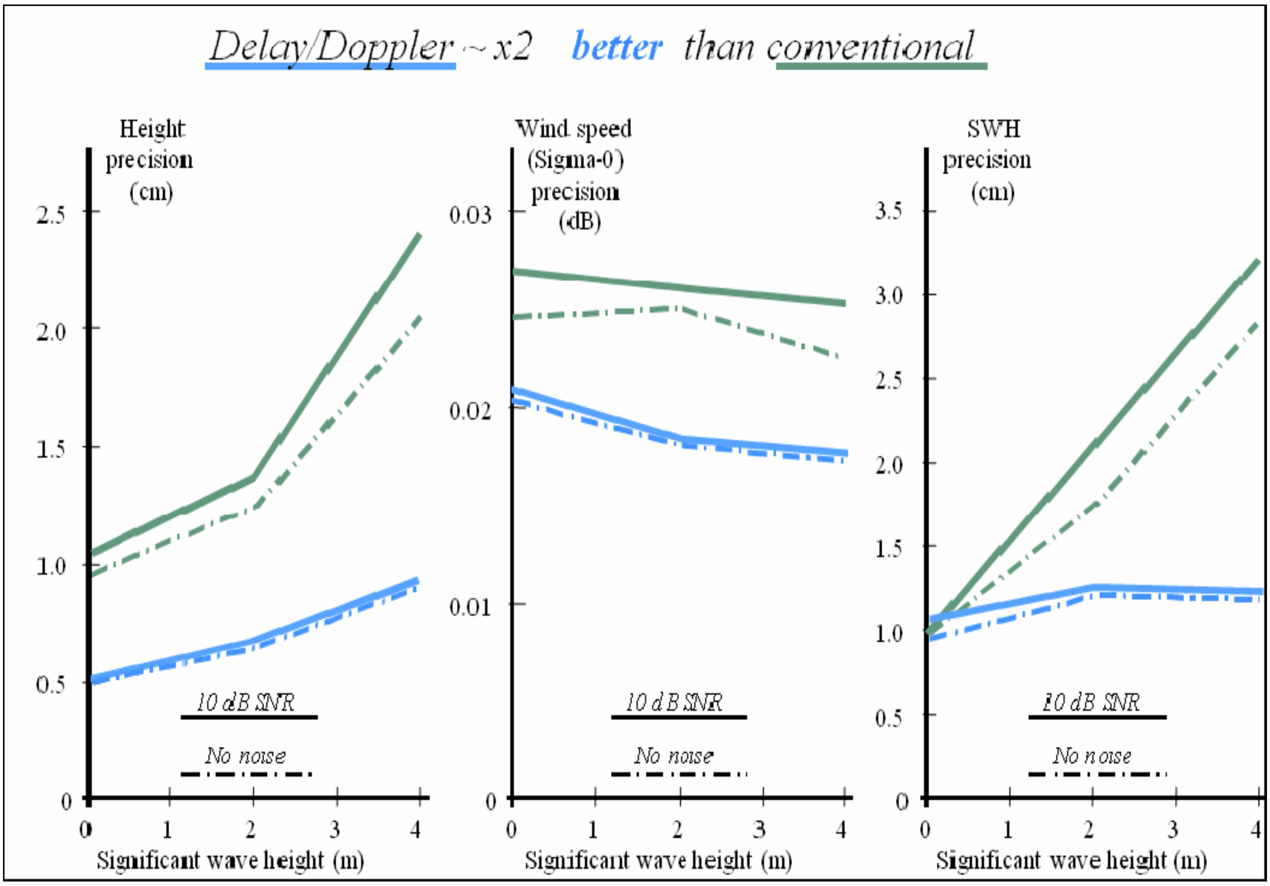


***Figure 1: Numerical estimates of the improved retrieval performance of Delay-Doppler Altimeters compared to conventional altimeters against SWH (Jensen & Raney, 1998)***

## 2. MOTIVATION

A major objective is to verify the improvement in sea surface height (SSH) measurement precision as a function of significant wave height (SWH) that has been predicted in theory as a benefit of a SAR mode radar altimeter. This verification was planned to be based on the analysis of actual data (such as should be available from CryoSat), and/or simulated data (as is available from the CRYMPS CryoSat simulator). This objective has not yet been achieved, but as summarized in this technical note, sufficient progress has been made such that strategies have been identified that when implemented will meet that objective.

Since CryoSat data will not be available in the near future, the initial verification exercises must rely on CRYMPS data. That implies that simulated data corresponding to the SAR mode and the LRM mode have to be compared quantitatively, for observations of the same input sea-state conditions. The simplest way to generate the required data is to run CRYMPS once over a given sea-state scenario, and to generate simultaneously two sets of output waveforms, one corresponding to a SAR mode data set, and the other corresponding to an LRM mode data set. (In the event that the "one run-two output" strategy is not feasible, equivalent data pairs could be obtained from two separate (SAR-mode and LRM-mode CRYMPS runs over identical input scenarios.) This technical note describes necessary steps to qualify CRYMPS data for quantitative mode comparisons, and offers recommendations for implementing said comparisons.

## 3. METHODOLOGY

The methodology for this work was specified explicitly in the ESA Statement of Work:

*"The study shall use simulated LRM data (at a PRF of 2 KHz) and SAR mode data (at a PRF of 18 KHz) over a simulated ocean surface with different SWH values."*

*"The data collected in SAR mode will be averaged to emulate a classical altimeter (pulse limited LRM mode). A software will need to be developed in order to reduce SAR mode data into pulse limited altimeter data for this purpose."*

*"The LRM and reduced SAR mode data will need to be retracked with a conventional ocean retracker."*

# 4. CRYMPS PRODUCTS AND SCENARIOS

The methodology in this WP is based on numerical simulations of CryoSat Low Resolution Mode (LRM) and SAR data products obtained from the CryoSat Mission Performance Simulator CRYMPS for a number of idealised Earth surface scenarios over open ocean.

## 4.1. CRYMPS

The CryoSat Mission Performance Simulator (CRYMPS) is a software tool used to simulate the CryoSat SIRAL echoes over configurable surfaces. CRYMPS was designed and developed by UCL/MSSL in collaboration with ESTEC as an end-to-end simulator for the SIRAL altimeter on the CryoSat mission.

## 4.2. SCENARIOS OVER OPEN OCEAN

CRYMPS has a number of configurable input parameters to customise the properties of the Earth surface. Primarily developed for exploitation over near-polar regions, these configurable input parameters were designed to describe ice surfaces. Nevertheless, in this study, the CRYMPS surface descriptors were examined and optimised to simulate conditions over open water surfaces. The scenarios and surface descriptors are shown in Table 1.

In the first instance, two idealised scenarios, F13 and F24, were formulated based on the most relevant of these existing input parameters, namely “swell” amplitude, “swell” wavelength and PDF standard deviation. By assigning values to these parameters, a surface Digital Elevation Map (DEM) is constructed, consisting of one sinusoid wave with specified “swell” amplitude and wavelength, superposed by normally distributed random noise with the specified PDF standard deviation. For F13, the “swell” characteristics were chosen to resemble the wind and wave conditions experienced during the CRYOVEX 2006 airborne experiment.

In the second instance, a more realistic description of sea state was adopted, whereby the full DEM was constructed at NOC, based on a theoretical Elfouhaily et al. (1997) ocean wave spectrum model. Two “real sea state” scenarios, SMC1 and SMC3, were requested, spanning SWH conditions ranging from 0 to 4 m, in steps of 1m. The DEM for SMC1 and SMC3 spanned 16 seconds along-track and are shown in Figure 2 and Figure 3.

## 4.3. CRYMPS ON-BOARD TRACKER

Ultimately, two versions of the CRYMPS products were obtained for each scenario, after artefacts were detected in the first runs linked to the onboard tracker in CRYMPS. The first set of runs made use of a “sensitive” on-board tracker optimised for ice surfaces; the second made use of a fixed onboard tracker. Results are shown for both versions.

| Code | Description | SWH | Swell Amplitude* | Swell wavelength* | PDF s.d.* | DEM by |
|---|---|---|---|---|---|---|
| **F13** | F1: CRYOVEX 2006, 02/05/2006<br>F3: CRYOVEX 2006, 30/04/2006 | 1.41m<br>0.71m | 1.0 m<br>0.5 m | 100 m<br>50 m | 4 cm<br>4 cm | MSSL |
| **F24** | F2: moderate sea state<br>F4: high sea state | 4.23 m<br>14.1 m | 3.0 m<br>10 m | 150 m<br>200 m | 10 cm<br>10 cm | MSSL |
| **C3** | Realistic ocean wave spectrum (Elfouhaily et al., 1997) | 1/2/3 m | N/A | N/A | 10 cm | NOC |
| **C1** | Realistic ocean wave spectrum (Elfouhaily et al., 1997) | 0.1/4/5 m | N/A | N/A | 10 cm | NOC |
| **FT1** | Sea Floor Topography 1, variations in sea surface height,<br>low SWH, short wavelength | 1.41 m | 1.0 m | 100 m | 4 cm | DNSC |

***Table 1: CRYMPS scenarios over open ocean. Parameters marked (*) are CRYMPS input parameters.***

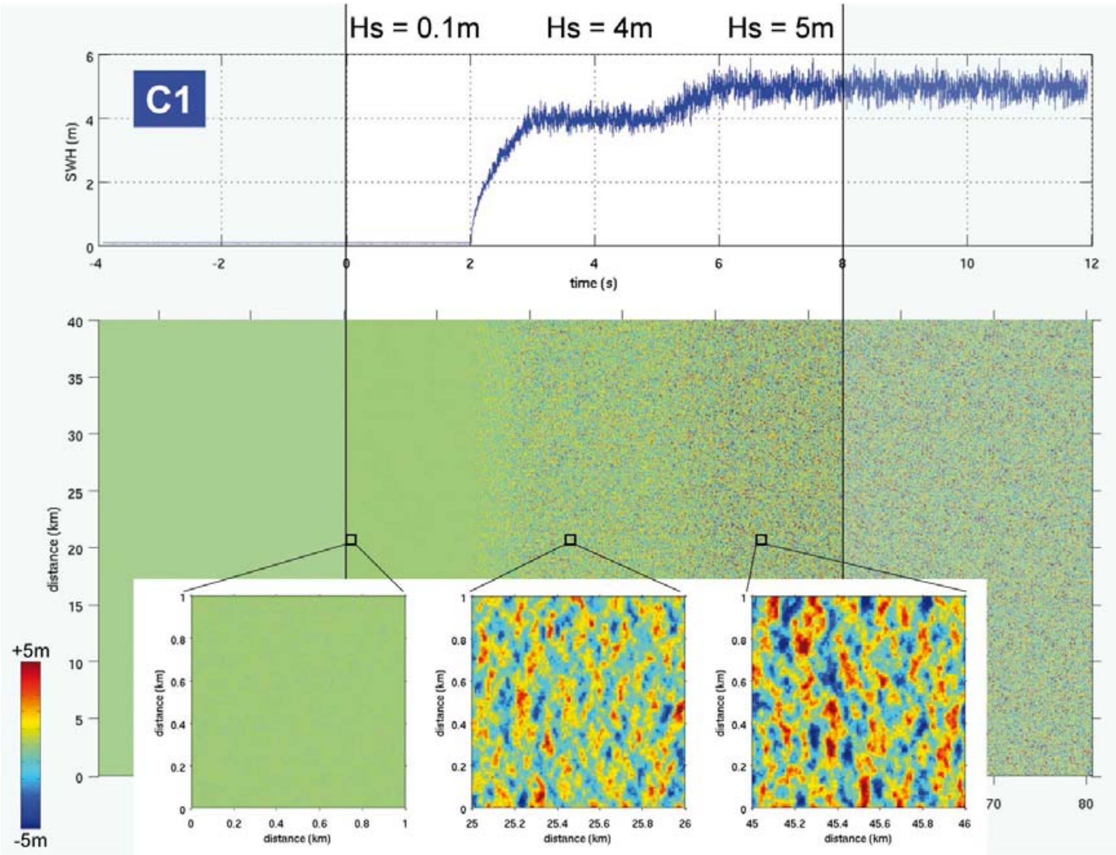


***Figure 2: Digital Elevation Map (DEM) for realistic ocean scenario SMC1***

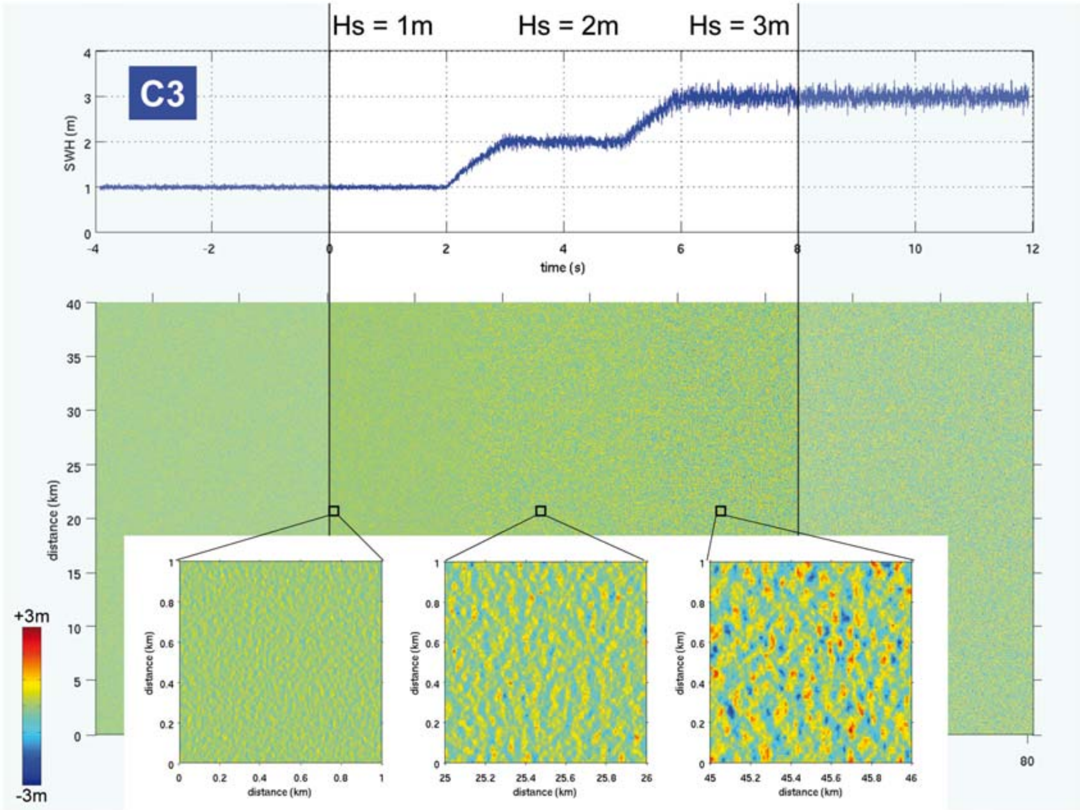


***Figure 3: Digital Elevation Map (DEM) for realistic ocean scenario SMC3***

5

# 5. SAR TO LRM REDUCTION SOFTWARE (RDSAR)

The CRYMPS output products consist of 18Hz Low Resolution Mode (LRM) waveforms and the SAR level 1 (or full bit rate data, FBR) data products. The SAR FBR data consists of complex waveforms (I and Q components). In SAR mode, the echoes must be SAR processed before incoherently multi-looking.

The sampling and averaging of the CRYMPS SAR products into 18Hz waveforms was performed by the RDSAR software produced by Starlab (for details, see Martin-Puig 2008a, 2008b, 2008c, 2008d).

Following some continuing uncertainty about the correct methodology to sample and average the CryoSat SAR data bursts into 18Hz waveforms, three versions of the RDSAR software have been produced to date. Only version 1 and version 3 of RDSAR were examined in this WP.

## 5.1. RDSAR_v.1

Version 1 of RDSAR software was delivered by Starlab on 14 February 2008. The sampling and averaging strategy of RDSAR_v1 had been described and agreed with ESA in a Technical Note issued by Starlab on 18 January 2008. The RDSAR_v1 processing was presented by Starlab at Progress Meeting #2 at NOCS on 12 March 2008.

The sampling and averaging strategy used in RDSAR_v1 is summarised in Figure 4 and Figure 5. It consist of a preliminary coherent pre-summing of 8 successive SAR waveforms in each burst, followed by incoherent averaging of the resulting pseudo-LRM waveforms (8 per burst) for 4 successive SAR bursts (total 32 pseudo-LRM waveforms) to form 18Hz averaged waveforms.

This scheme exploits the complete set of SAR waveforms available in any 18Hz period, i.e. 4*64 = 256 waveforms.

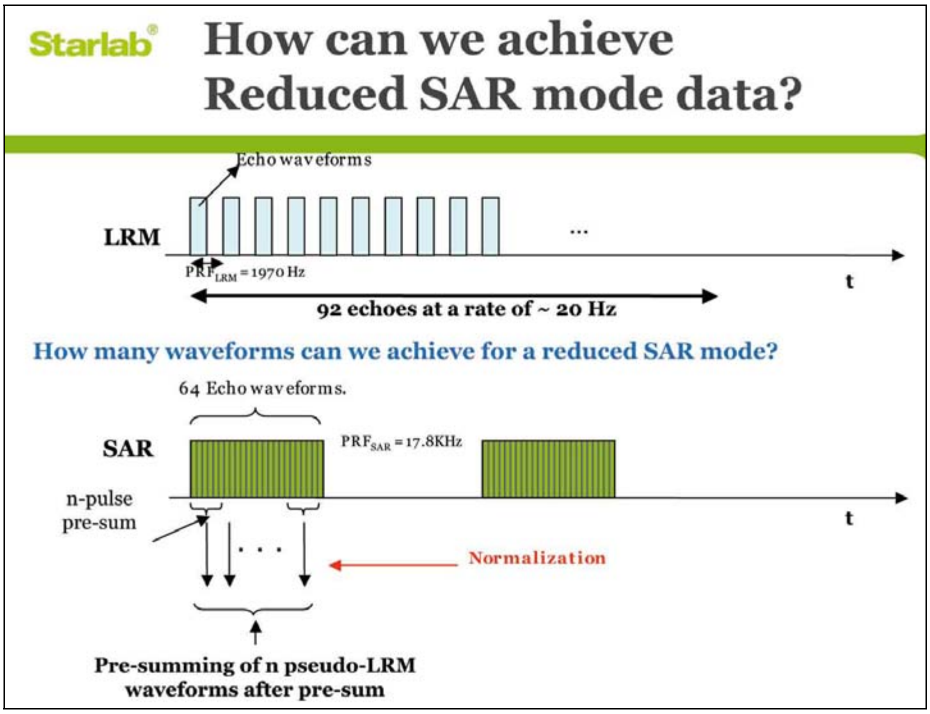


***Figure 4: Sampling and averaging strategy in RDSAR Version 1 (as presented by Cristina Martin-Puig, Progress Meeting #2, NOCS, 12 March 2008)***

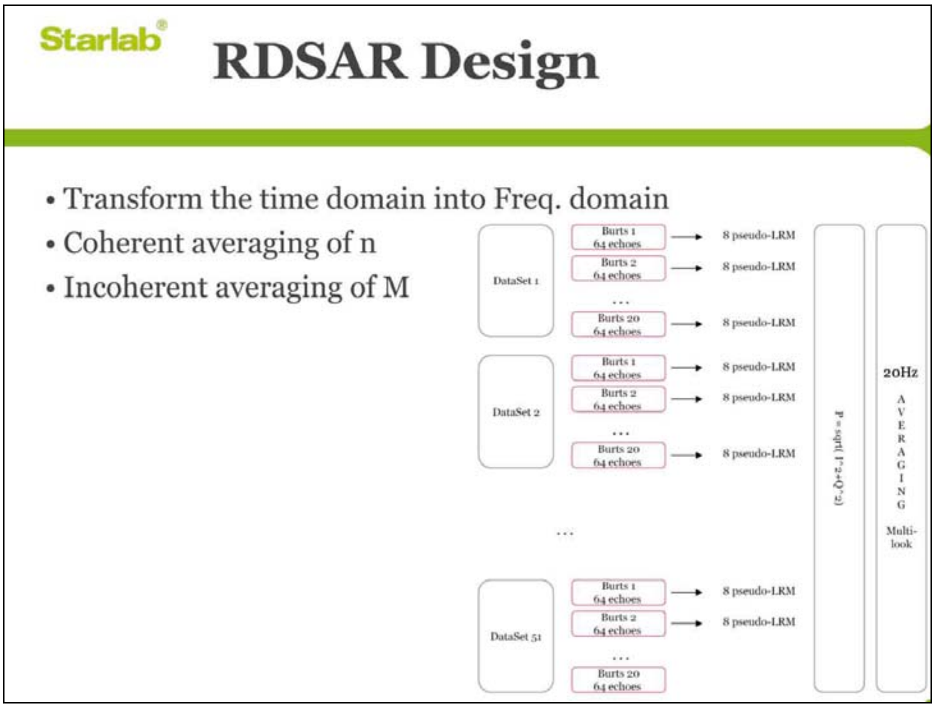


***Figure 5: SAR to LRM reduction scheme in RDSAR Version 1 (as presented by Cristina Martin-Puig, Progress Meeting #2, NOCS, 12 March 2008)***

## 5.2. RDSAR_v.2

Version 2 of the RDSAR software was produced by Starlab on 27 March 2008 but, following discussions within the team, was quickly superseded by version 3. Version 2 of RDSAR was therefore not implemented for the following analyses.

## 5.3. RDSAR_v.3

Version 3 of the RDSAR software was delivered by Starlab on 10 April 2008. The sampling and averaging strategy used in RDSAR_v3 is summarised in Figure 6.

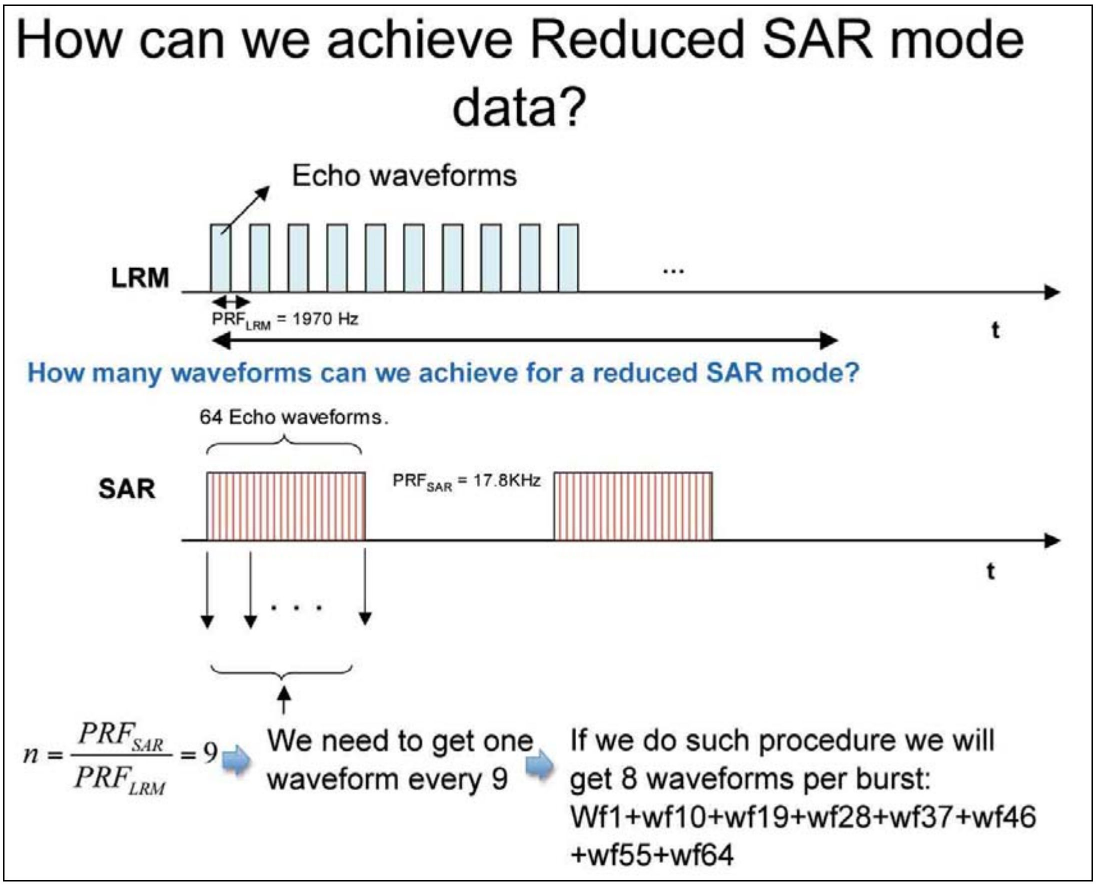


***Figure 6: Sampling and averaging strategy in RDSAR Version 3 (courtesy of Cristina Martin-Puig, by email, 10 April 2008)***

The new sampling and averaging strategy now uses only 1 in every 9 SAR FBR echoes and does not perform any coherent averaging.

Contrary to RDSAR_v1, RDSAR_v3 now exploits only 1 in every 9 SAR waveforms in any 18Hz period, i.e. 8*4 = 32 waveforms.

# 6. LRM, RDSAR and Ocean retracker processing chain

## 6.1. Software processing chain

The chain of software tools required to process the LRM and RDSAR products is illustrated in Figure 7. These results were presented by NOCS at Progress Meeting #2 at NOCS on 12 March 2008.

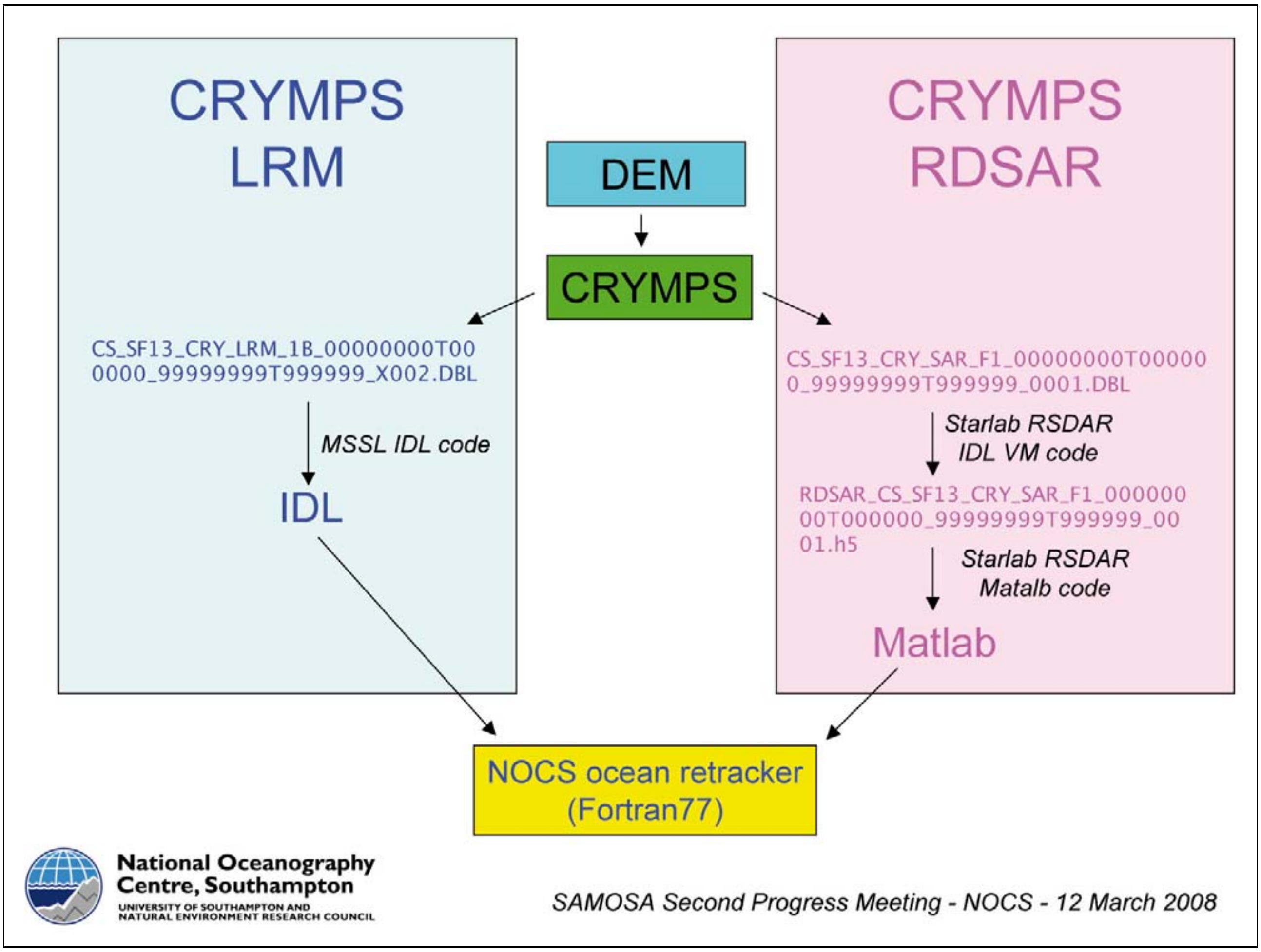


***Figure 7: Chain of software tools for the processing and analysis of CRYMPS LRM and RDSAR waveforms.***

In what follows, we present for each of the open ocean scenario, SF13, SF24, SMC1, SMC3 and SFT1:

- The LRM waveforms
- The RDSAR output waveforms
- The NOCS ocean retracker results for LRM waveforms
- The NOCS ocean retracker results for RDSAR waveforms.

## 6.2. CRYMPS LRM & RDSAR PRODUCTS

The LRM and RDSAR figures show all waveforms present in the CRYMPS LRM and RDSAR products for each scenario. The waveforms are displayed as scaled intensity (z-axis) plotted against along-track sample number (x-axis) and waveform gate number (y-axis).

In the case of the LRM products, there are 260 samples in each product, which, assuming these correspond to 18Hz averages, correspond to 14.4 seconds along-track (out of the 16 second DEM provided). Since no information was available on how to scale the waveform intensity into power, the analyses were performed on digital numbers scaled by $10^6$.

In the case of RDSAR products, there are 250 samples per product, which assuming these correspond to 18Hz averages, correspond to 13.9 seconds along-track (out of the 16-second DEM provided). As for LRM, the waveform intensity could not be scaled into power for lack of information, and the analyses were performed on un-scaled waveform intensity.

## 6.3. NOCS OCEAN RETRACKER

The NOCS ocean retracker was applied to both 18Hz LRM and RDSAR waveforms for all scenarios. The ocean retracker consists of a theoretical Brown ocean model, implemented here in its 4-parameter retrieval mode (thermal noise, SWH, epoch, Sigma0), using least-square fitting and Gaussian wave statistics. The figures relating to the ocean retracker results show the retrieved parameters plotted along-track in 5 subplots corresponding to (from top to bottom):

- Retrieved SWH
- Sigma0 (aka Normalised Radar Cross Section): the retrieval of this parameter was prevented by the absence of information on waveform power scaling.
- Epoch (related to the range)
- Thermal noise
- Retrieval quality flag: provides information of the quality of the retrieval, with larger values of the flag suggesting poorer model-data fits.

## 6.4. RESULTS OUTLINE

In what follows we show:

- A short synthesis and discussion of the “Results Version 1” in Section 7.
- Results Version 2 (CRYMPS/Fixed Tracker & RDSAR_v.3) for scenario SMC1 and SMC3, including a preview of the LRM waveforms for SF13, SF24 and SFT1.
- A discussion of all results in Section 9.

# 7. RESULTS VERSION 1: CRYMPS RUNS (ICE TRACKER) & RDSAR_V1

Results Version 1 (hereafter, RV1) refer to the results obtained with Version 1 of the CRYMPS runs (ice tracker – see section 4.3) and Version 1 of the RDSAR software (see section 5).

## 7.1. ARTEFACTS IN RV1 RESULTS

The RV1 results for all scenarios are shown in Annex A. From these results, we observe that:

- Except for SF13, all scenarios display unexpected crenellations at the leading edge, probably related to the behaviour of the CRYMPS ice tracker over sections of the scenarios with rapid SWH changes. This is particularly striking for scenario SF24. Also, the number and location of Artefacts can differ in the LRM and RDSAR waveforms for the same scenario e.g. SMC3.

- In all cases, the crenellations appear shifted along-track in the RDSAR products compared to LRM, suggesting that the RDSAR and LRM products do not correspond exactly to the same section of the DEM. This will make it difficult to confidently identify the sections of the runs relevant to given SWH conditions. Unfortunately, contrary to LRM, the RDSAR products do not preserve the CRYMPS along-track time or latitude/longitude information.

- The RDSAR waveforms appear very "peaky" and lack the trailing edge plateau expected in Brown-type ocean waveforms. It is suggested that this is a residual effect of the way the coherent integration was performed in RDSAR_v1.

## 7.2. NOCS OCEAN RETRACKER RESULTS FOR RV1

Both LRM and RDSAR waveforms were successfully retracked by the NOCS ocean retracker in all scenarios. However, the larger values of retrieval confidence flag (ifail flag, bottom subplots) indicate that retrieval is generally unsatisfactory in the RDSAR cases. This is consistent with point 3 above.

While the NOCS ocean retracker was able to retrieve SWH values consistent with the original DEM SWH for LRM waveforms, this was not so for RDSAR. Figure 8 shows the DEM SWH for SMC1 and SMC3, while Figure 9 summarise the retrieved SWH for LRM and RDSAR for the same scenarios. Figure 10 shows the equivalent plot for the retrieved epoch.

Even notwithstanding the large artefacts seen in the retrieved range, it is difficult to see from the retrieved SWH how to identify the sections of the RDSAR runs corresponding to different SWH conditions. As a result of these uncertainties, we were not able to compute the range retrieval error versus SWH in LRM and RDSAR.

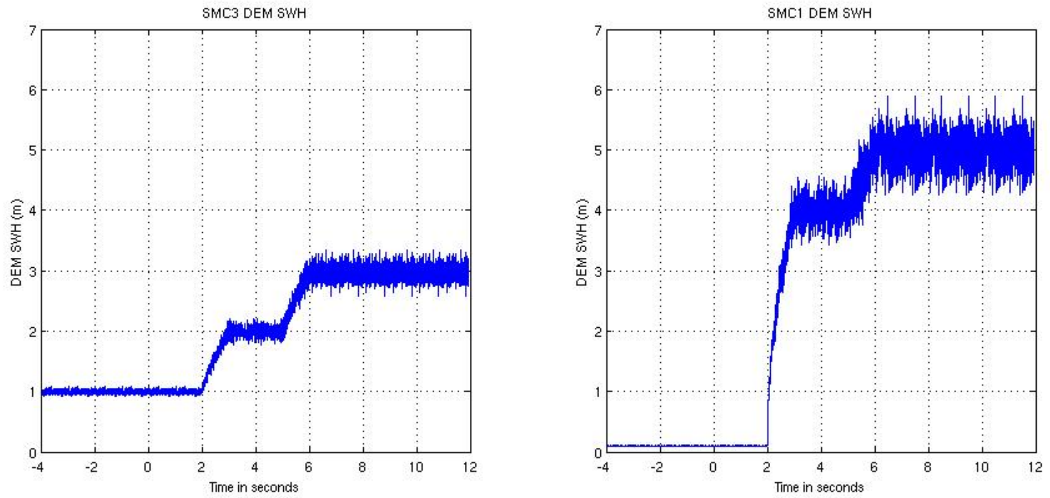


***Figure 8 – Evolution of the DEM SWH in realistic open ocean scenarios SMC3 (left) and SMC1 (right)***

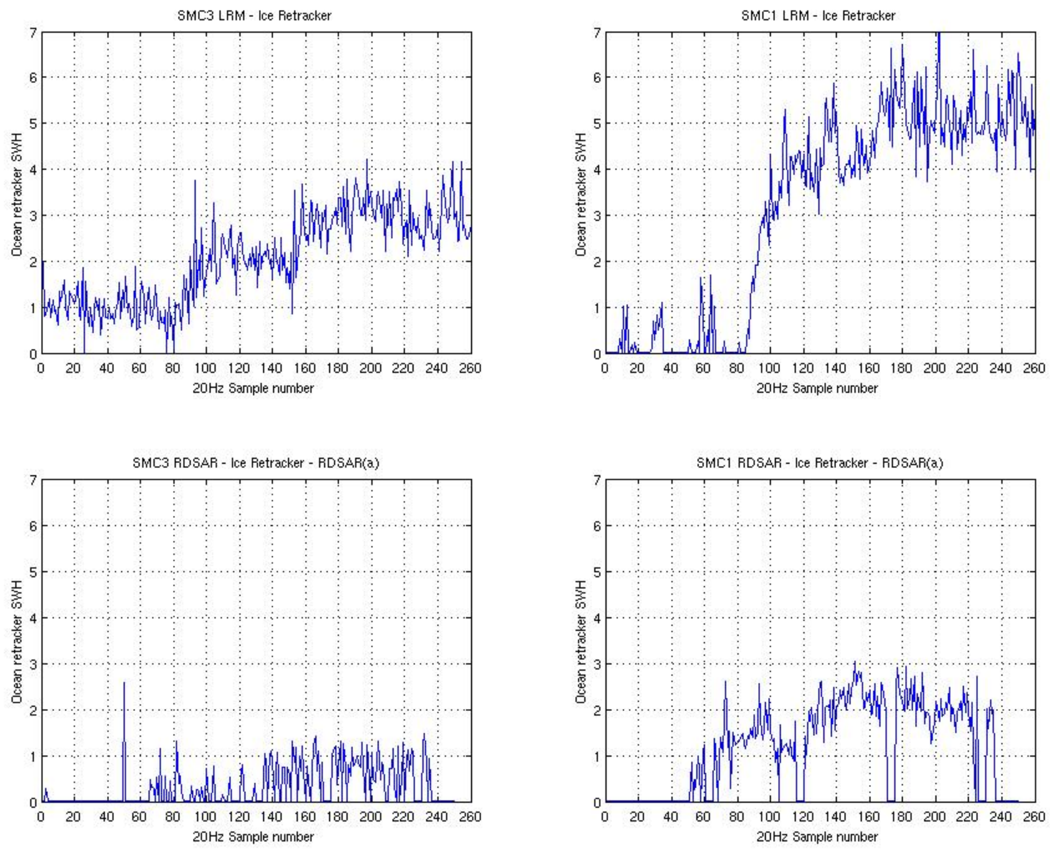


***Figure 9 – NOCS ocean retracker retrieved SWH for the realistic open ocean scenarios SMC3 (left) and SMC1 (right) in the case of LRM (top) and RDSAR (bottom) waveforms (RV1)***

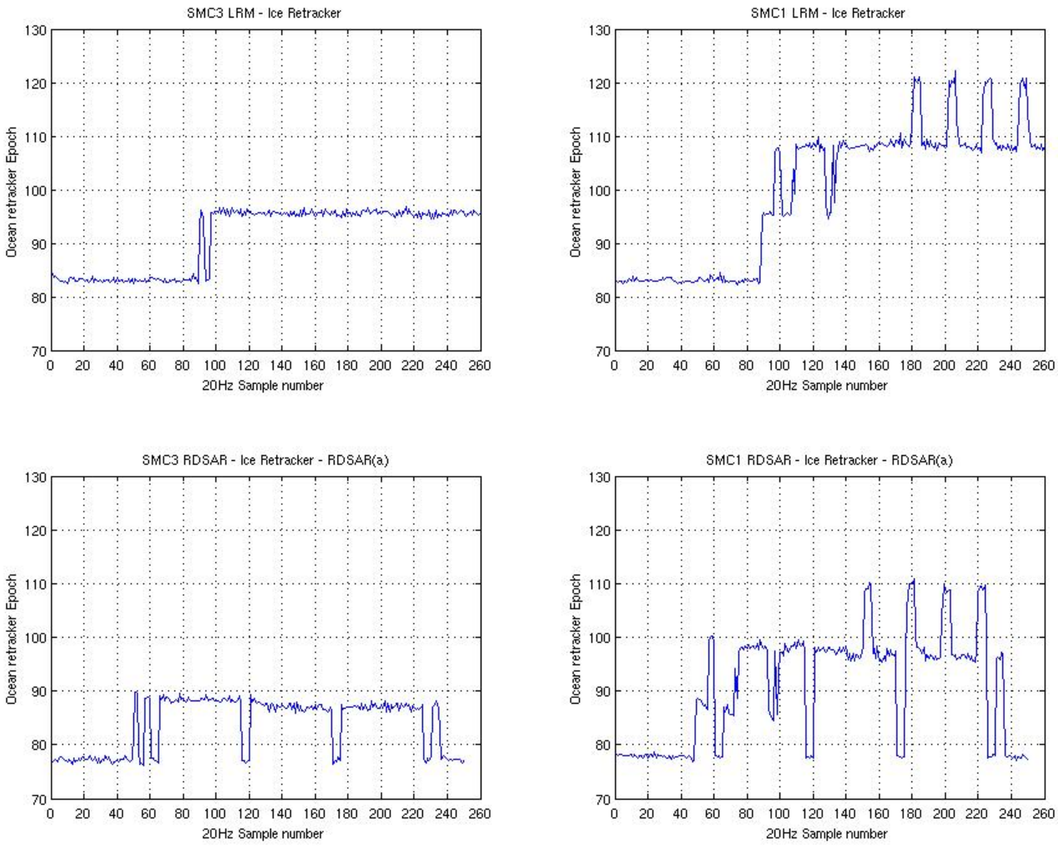


***Figure 10 - NOCS ocean retracker retrieved epoch for the realistic open ocean scenarios SMC3 (left) and SMC1 (right) in the case of LRM (top) and RDSAR (bottom) waveforms (RV1).***

## 8. RESULTS VERSION 2: CRYMPS/FIXED TRACKER & RDSAR_V.3

Results Version 2 (hereafter, RV2) refer to the results obtained with Version 2 of the CRYMPS runs (fixed tracker – see Section 4.3) and Version 3 of the RDSAR software (see Section 5). These results were presented by NOCS as an oral presentation at the EGU General Assembly 2008 on 16 April 2008 (Gommenginger et al., 2008).

Due to limited effort remaining to complete this work, the RDSAR and ocean retracking analyses were repeated in RV2 only for the realistic open ocean scenarios, namely SMC1 and SMC3. We begin by presenting the LRM, RDSAR and ocean retracking results for SMC1 and SMC3. The LRM waveforms were examined in RV2 for all 5 scenarios and are provided here in Section 8.3 for completeness.

## 8.1. SMC1 (RV2)

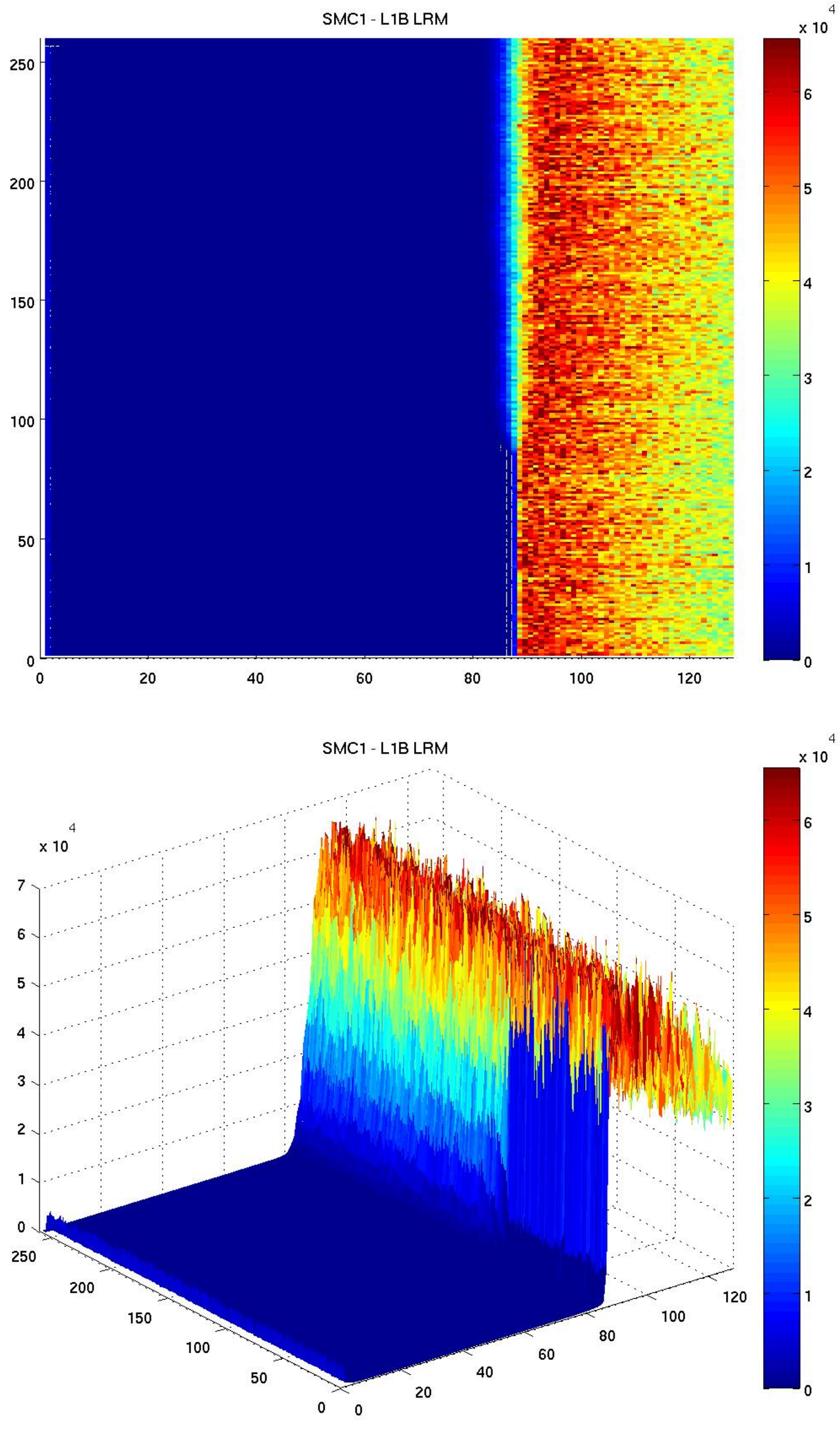


***Figure 11 – CRYMPS Low-Resolution Mode (LRM) waveforms for open ocean scenario SMC1 (RV2)***

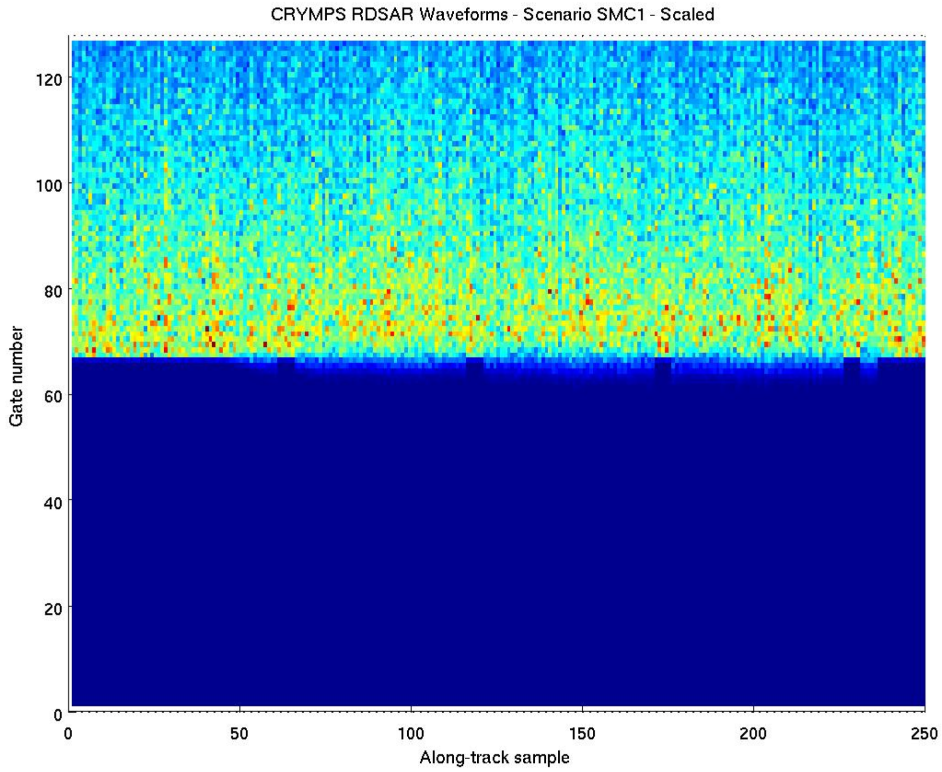


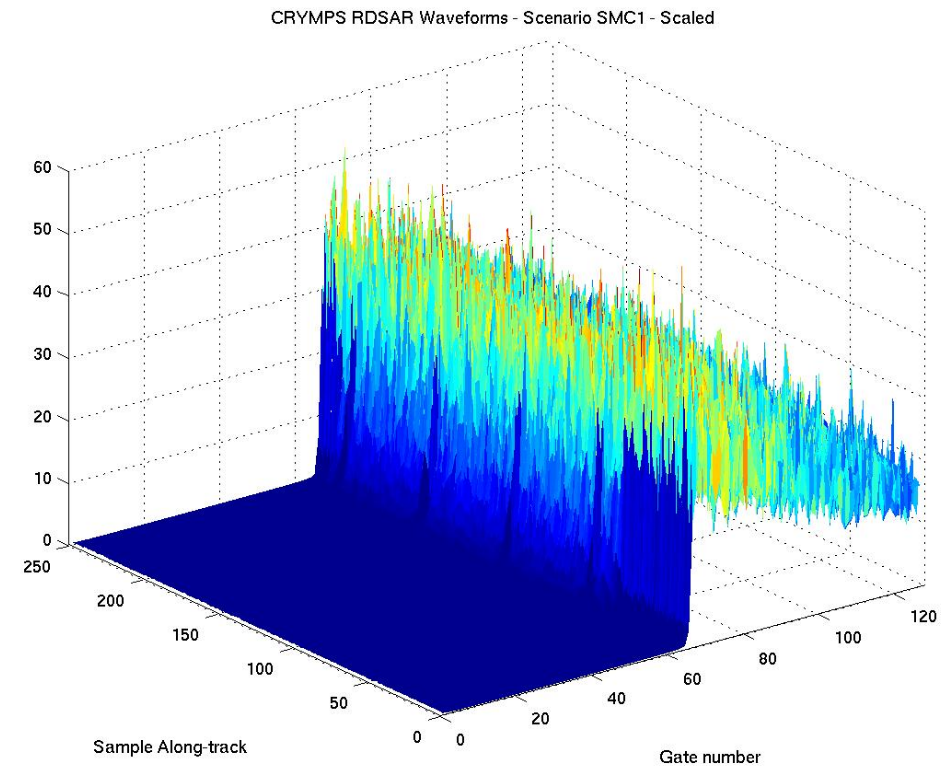


***Figure 12 – CRYMPS Reduced SAR (RDSAR) waveforms for open ocean scenario SMC1 (RV2)***

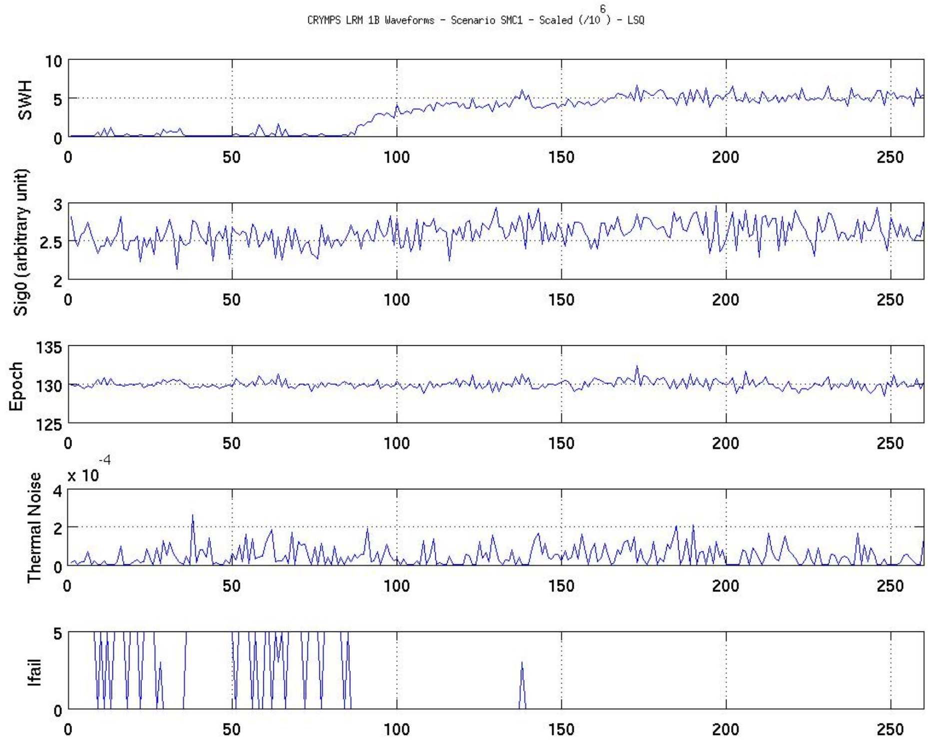


***Figure 13 – NOCS ocean retracker (top to bottom) retrieved SWH, Sigma0, epoch, thermal noise and retrieval quality flag for CRYMPS LRM waveforms (scaled by $10^6$) for open ocean scenario SMC1 (RV2).***

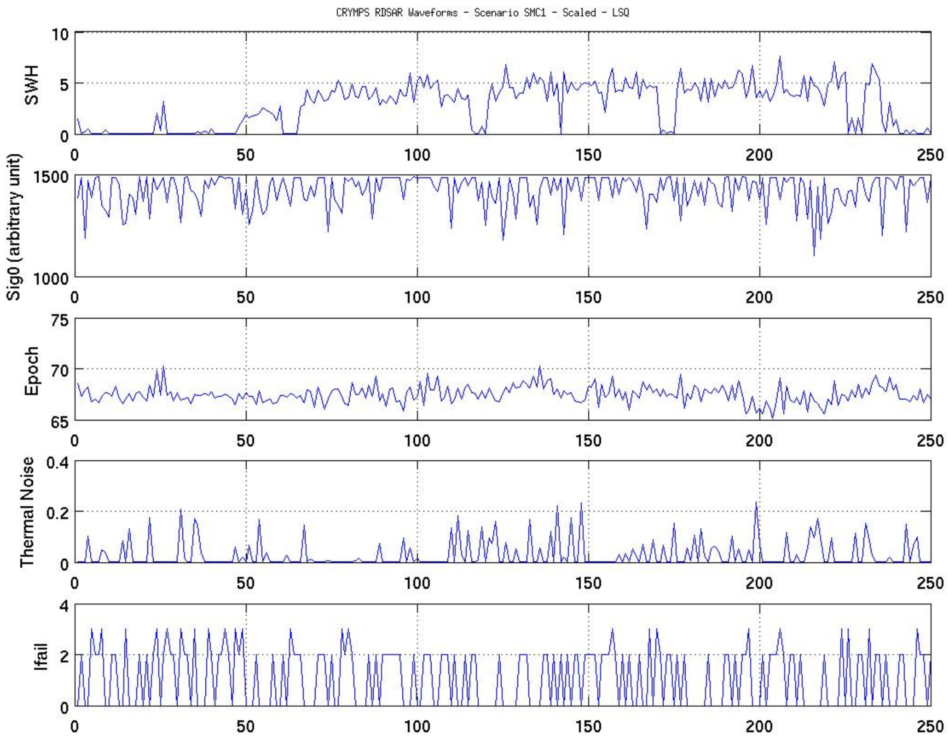


***Figure 14 – NOCS ocean retracker (top to bottom) retrieved SWH, Sigma0, epoch, thermal noise and retrieval quality flag for CRYMPS RDSAR waveforms (scaled by 1, i.e. unscaled) for open ocean scenario SMC1 (RV2).***

## 8.2. SMC3 (RV2)

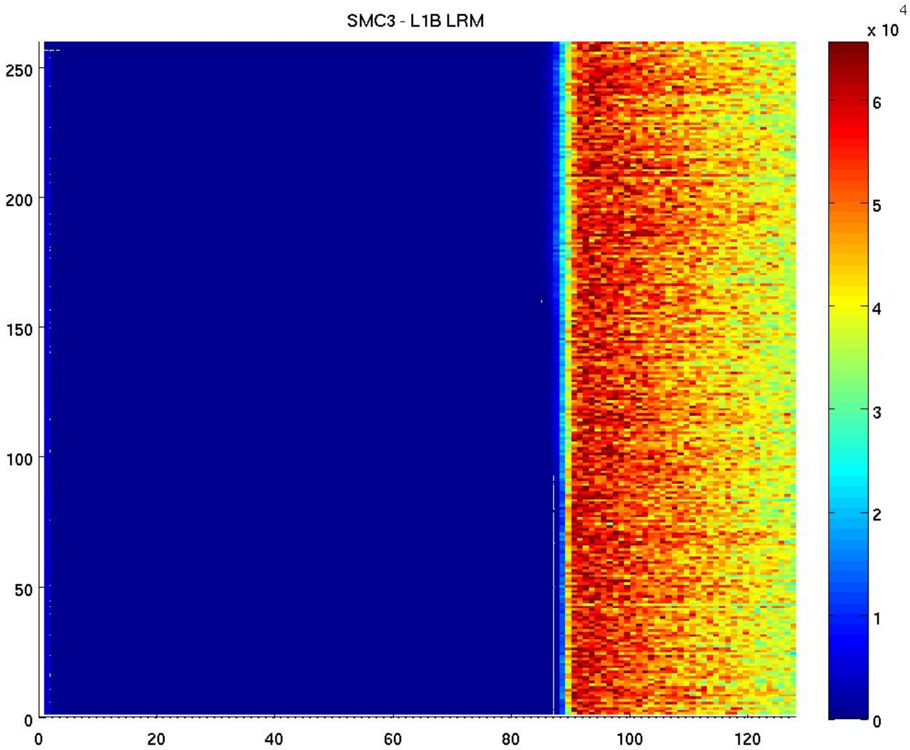


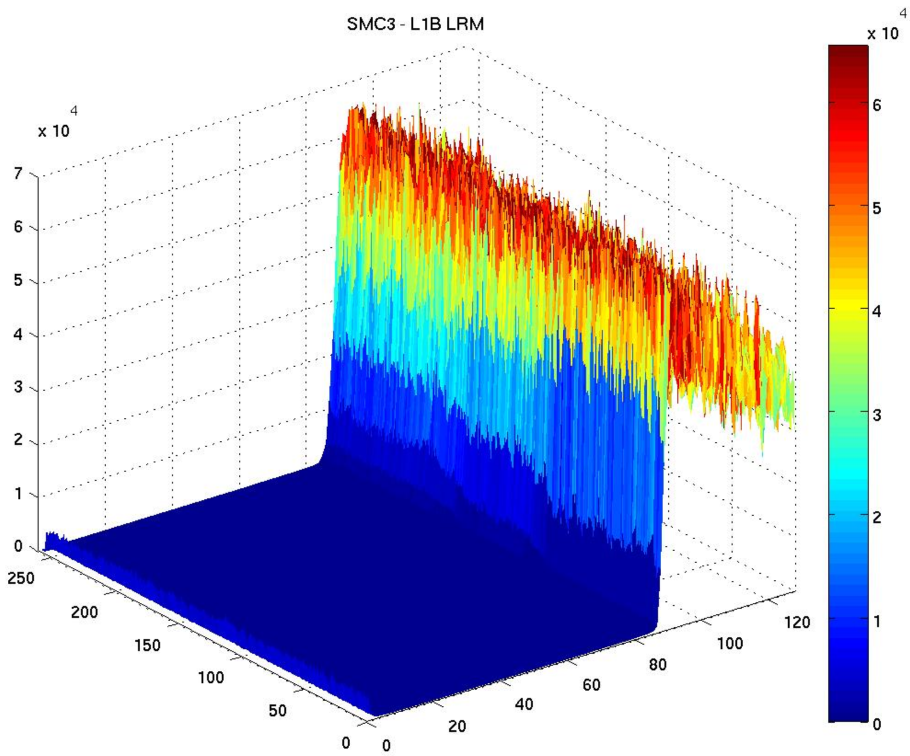


***Figure 15 – CRYMPS Low-Resolution Mode (LRM) waveforms for open ocean scenario SMC3 (RV2)***

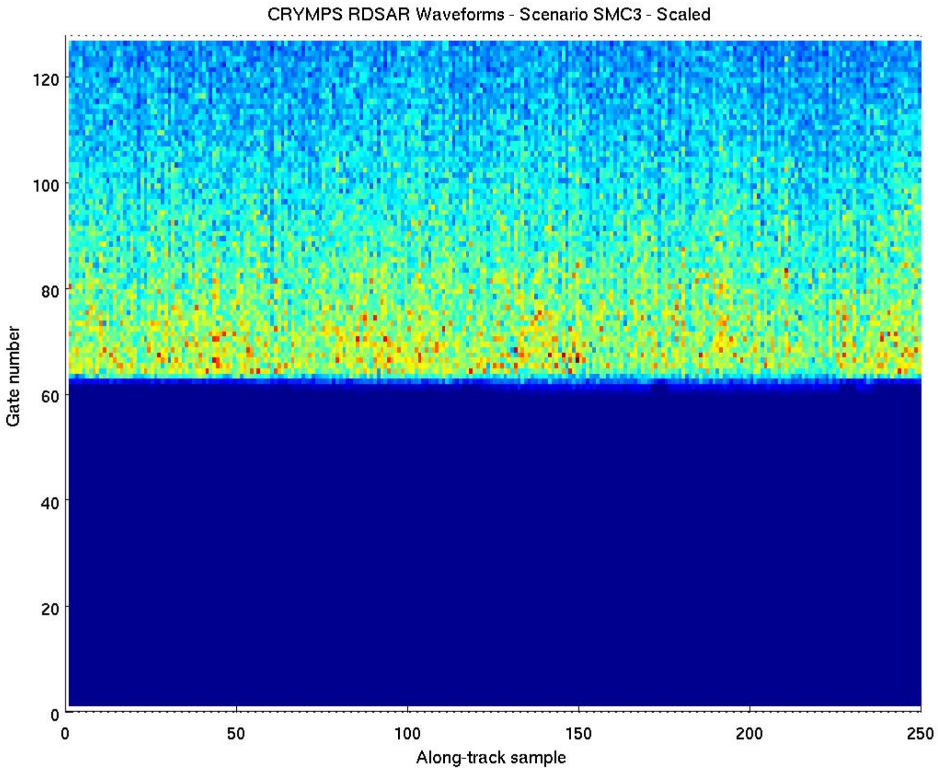


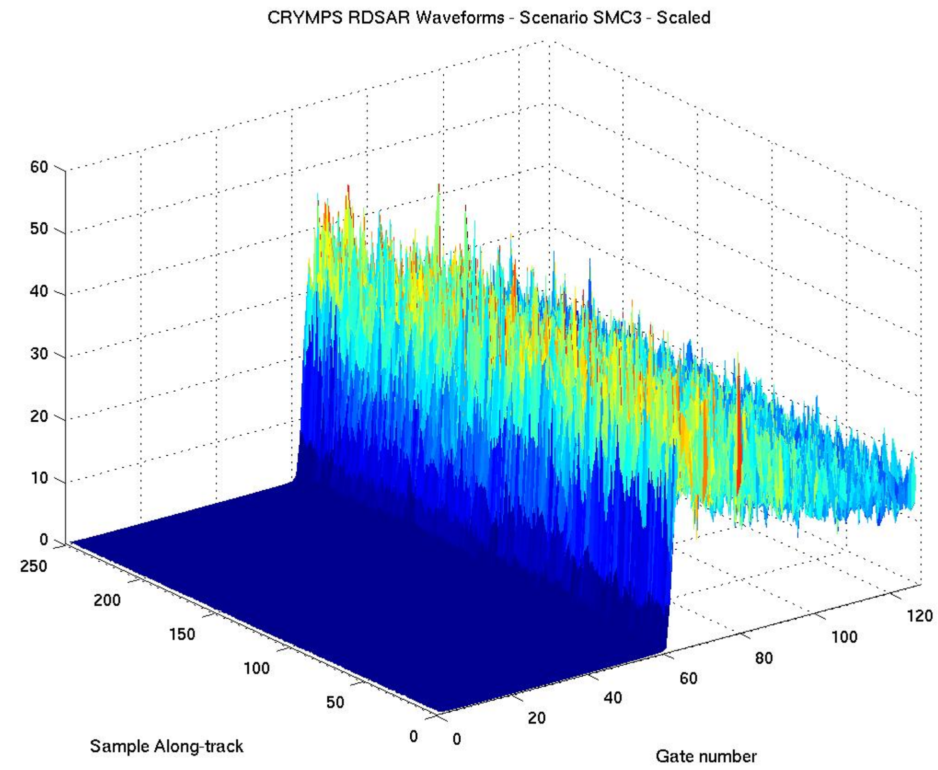


***Figure 16 – CRYMPS Reduced SAR (RDSAR) waveforms for open ocean scenario SMC3 (RV2)***

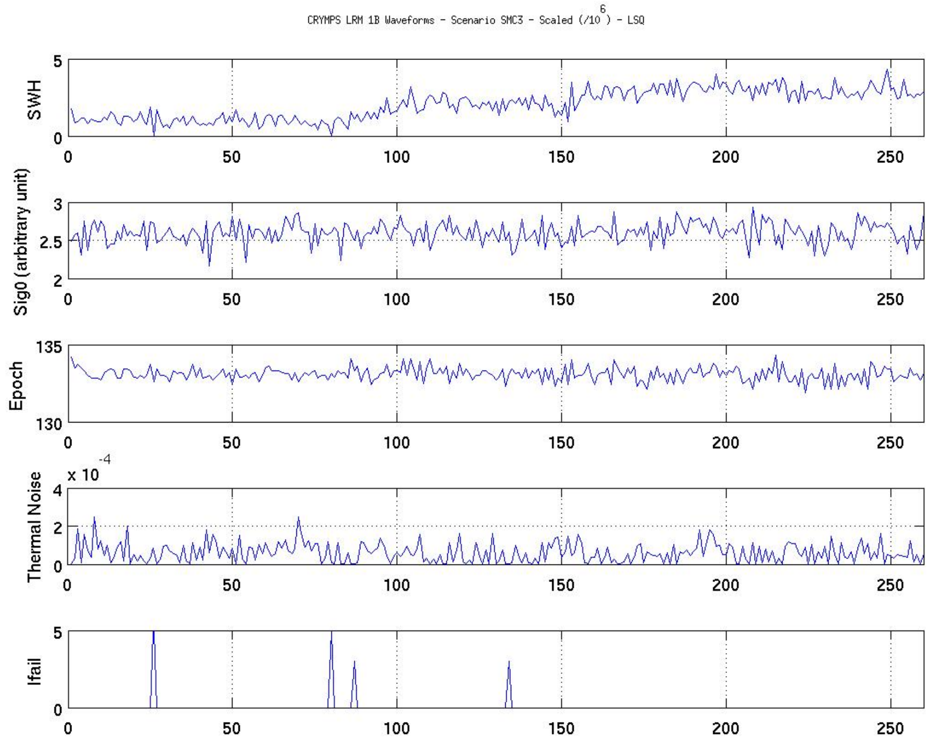


***Figure 17 – NOCS ocean retracker (top to bottom) retrieved SWH, Sigma0, epoch, thermal noise and retrieval quality flag for CRYMPS LRM waveforms (scaled by $10^6$) for open ocean scenario SMC3 (Version 2).***

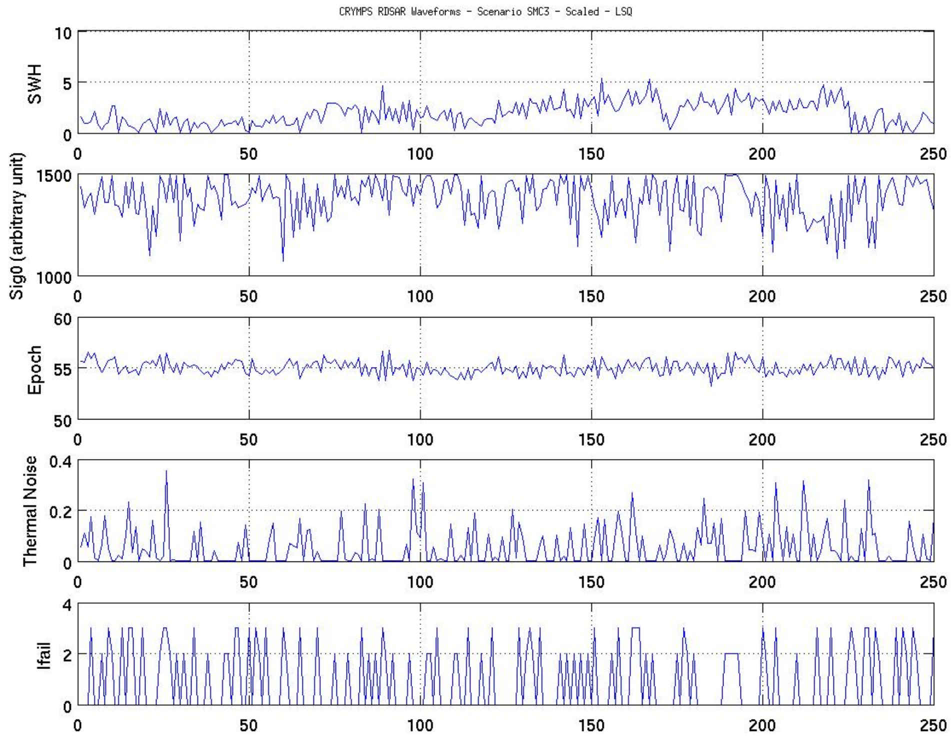


***Figure 18 – NOCS ocean retracker (top to bottom) retrieved SWH, Sigma0, epoch, thermal noise and retrieval quality flag for CRYMPS RDSAR waveforms (scaled by 1, i.e. unscaled) for open ocean scenario SMC3 (Version 2).***

## 8.3. LRM RESULTS FOR SF13, SF24 AND SFT1 (RV2)

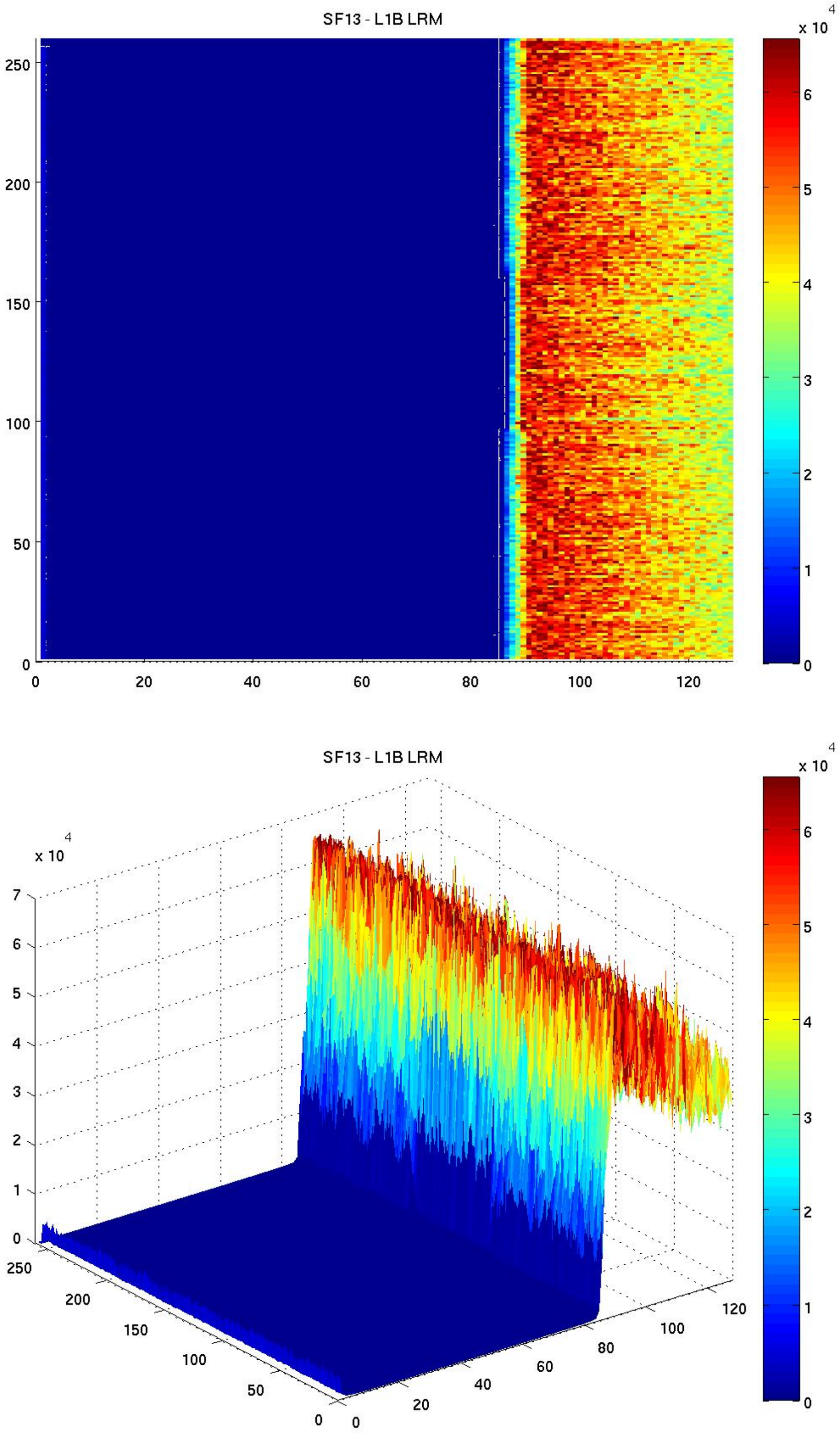


***Figure 19 – CRYMPS Low-Resolution Mode (LRM) waveforms for open ocean scenario SF13 (RV2)***

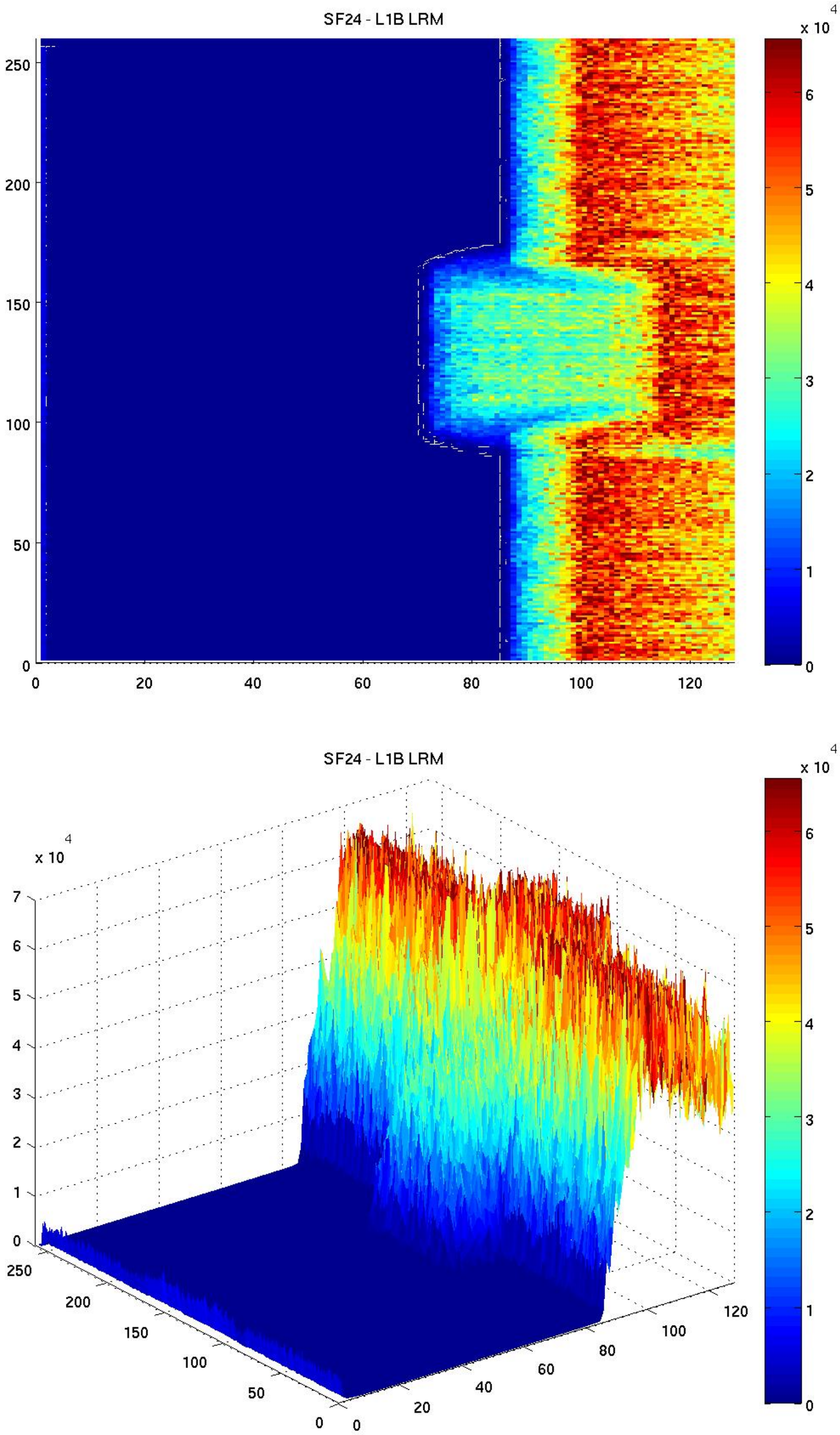


***Figure 20 – CRYMPS Low-Resolution Mode (LRM) waveforms for open ocean scenario SF24 (RV2)***

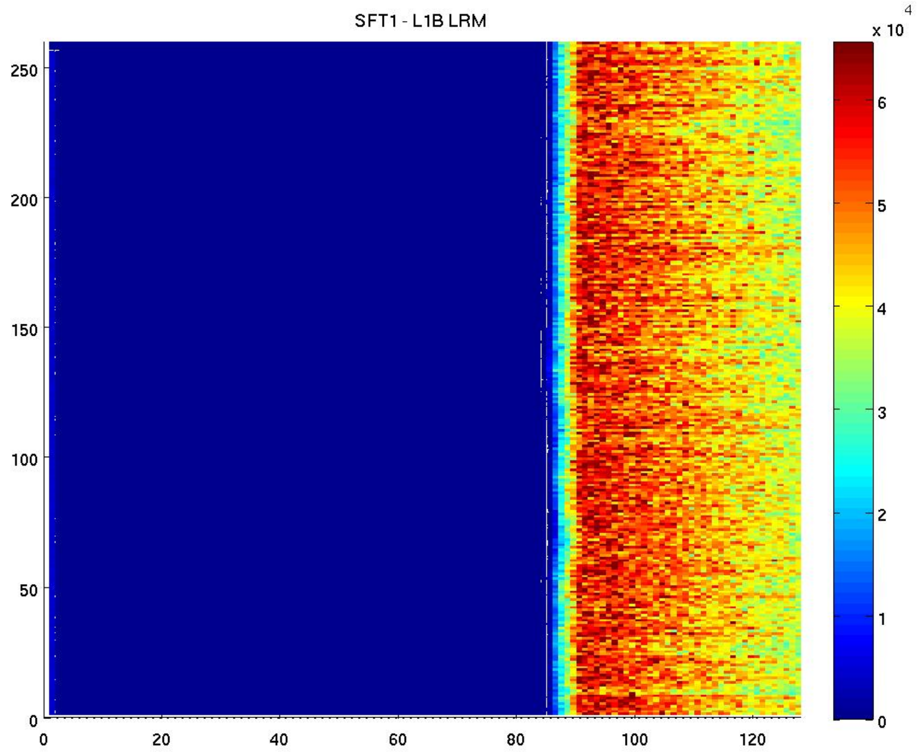


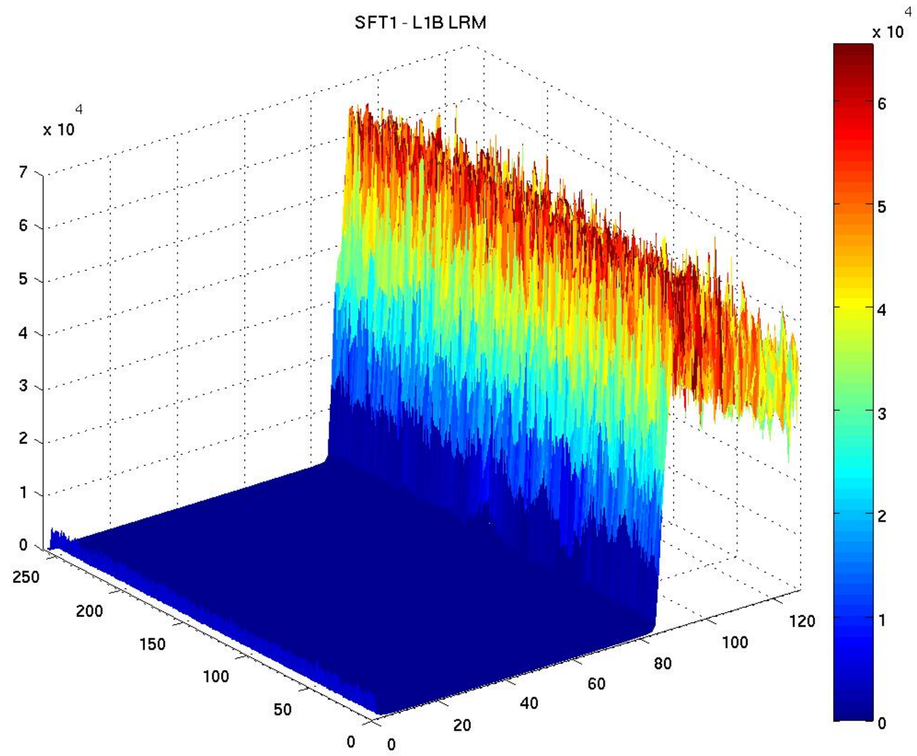


***Figure 21 – CRYMPS Low-Resolution Mode (LRM) waveforms for open ocean with bathymetry scenario SFT1 (RV2)***

# 9. SYNTHESIS AND DISCUSSION OF RV2 RESULTS

## 9.1. RV2 RESULTS

From these RV2 results, we observe that:

- Except for SF24, the crenellations at the leading edge have disappeared from all LRM products for all scenarios. Some minor crenellations remain in the RDSAR products for SMC1 (see Figure 12 and Figure 14, top plot).

- The peakiness of the RDSAR waveforms has disappeared and the RDSAR waveforms now conform to the Brown-type ocean waveform shape, with a clear trailing edge plateau.

## 9.2. NOCS OCEAN RETRACKER RESULTS FOR RV2

Both LRM and RDSAR waveforms were successfully retracked by the NOCS ocean retracker for SMC1 and SMC3. However, the retracker still returns larger values of retrieval confidence flag (ifail flag, bottom subplots) in the case of RDSAR, thereby indicating that the retrieval remains poorer for RDSAR than LRM. This is likely to be due to the smaller number of waveforms averaged in RDSAR (32) than in LRM (~92).

The NOCS ocean retracker was again able to retrieve for the LRM waveforms SWH values consistent with the original DEM SWH for scenarios SMC1 and SMC3. This is seen clearly in Figure 22 and Figure 23 (top subplots). The increase in the variability of the LRM retrieved SWH and range for higher values of SWH is visible by eye in Figure 23 and Figure 24. The LRM retrieved SWH in SMC1 and SMC3 in RV2 are quasi-identical to the results obtained in RV1.

The RDSAR retrieved SWH are closer to the DEM SWH in RV2 than in RV1, but are very noisy. The RDSAR SWH display large spikes and rapid drop-outs, both in SMC3 and SMC1, reminiscent of the crenellations seen in RV1. The rapid SWH transition from 0 to 4 m in SMC1 occurs at a different position in the LRM and RDSAR products, indicating that the along-track shift between the sections of the DEM depicted by LRM and RDSAR products has not been resolved. In these conditions, it remains difficult to identify in Figure 23 and Figure 24, which sections of the RDSAR runs correspond to different SWH conditions. The final plot of range (and SWH) retrieval error versus SWH for LRM and RDSAR could therefore not be computed.

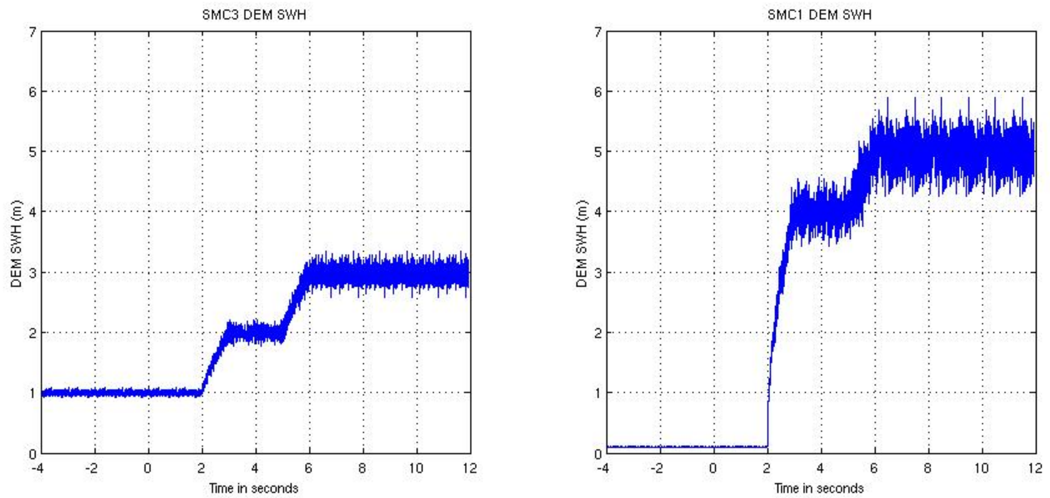


***Figure 22: Evolution of the DEM SWH in realistic open ocean scenarios SMC3 (left) and SMC1 (right) (same as Figure 8)***

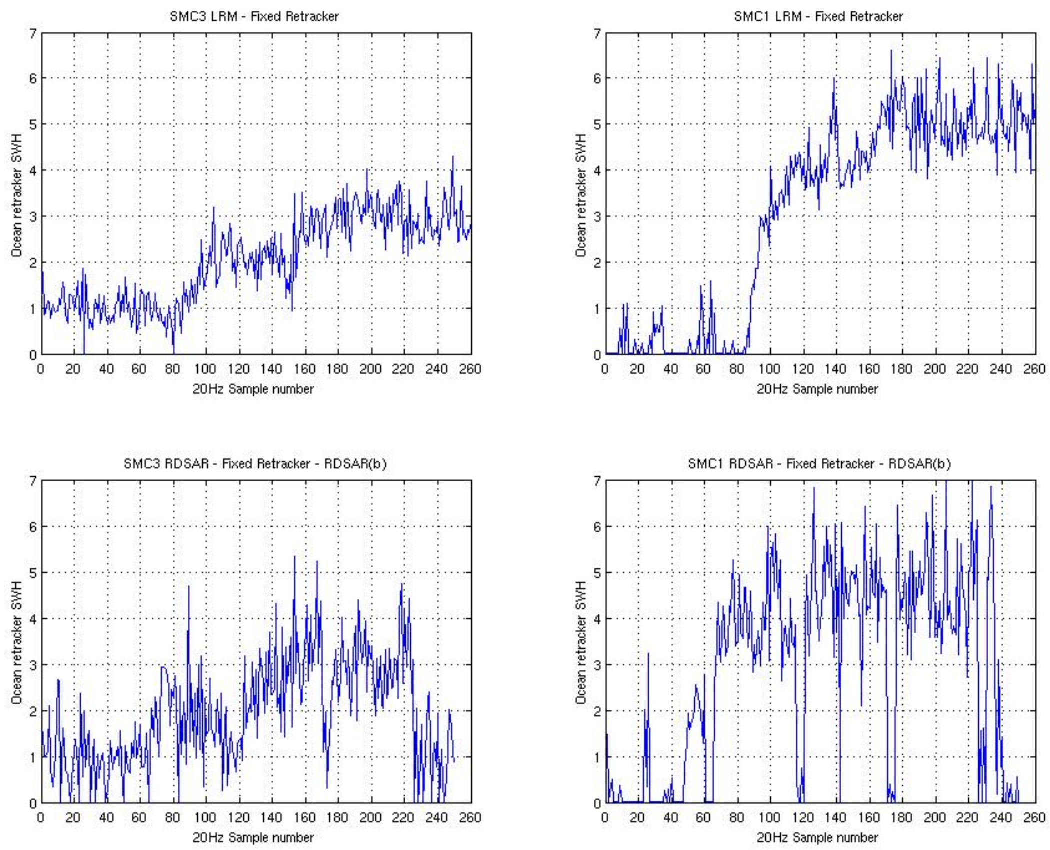


***Figure 23 – NOCS ocean retracker retrieved SWH for the realistic open ocean scenarios SMC3 (left) and SMC1 (right) in the case of LRM (top) and RDSAR (bottom) waveforms (RV2)***

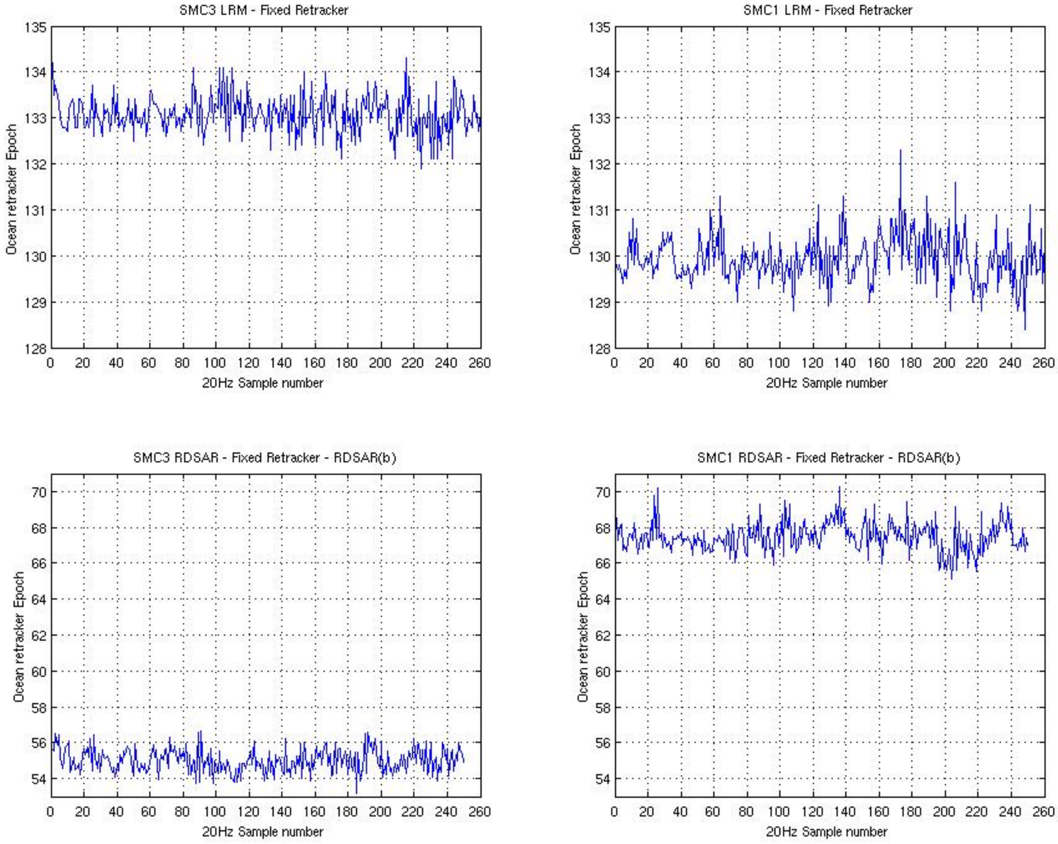


***Figure 24 - NOCS ocean retracker retrieved epoch for the realistic open ocean scenarios SMC3 (left) and SMC1 (right) in the case of LRM (top) and RDSAR (bottom) waveforms (RV2).***

# 10. GENERAL DISCUSSION

As detailed in the report, the sea surface sampling schemes for the two CryoSat modes differ significantly. Thus, it has proven to be not straightforward to generate reasonable pseudo-LRM mode data from the (simulated) SAR mode data. The results from RDSAR Version 1 and Version 3 have raised as many questions as answers.

Of more general interest is the lingering question whether CRYMPS data are up to the task of supporting quantitative mode-to-mode comparisons, based on transforming SAR-mode data to pseudo-LRM mode data. Two logical experiment classes are required to address this issue: (1) qualification of CRYMPS data (the “control” experiment”), and (2) quantified comparison of the measurement precision of the two modes (the “verification” experiment). In other words, before verification, the basic suitability of CRYMPS data products for comparisons must be established. One approach to the required control experiment for CRYMPS data is outlined in the Recommendations section of this Technical Note. Once CRYMPS data are so qualified, then there are robust options for moving ahead with the intended comparison of the two modes. Again, one approach is outlined in the Recommendations section.

Given the logical equivalence between the simulated and the actual SAR mode data, the value of a verified methodology of generating pseudo-LRM data from the SAR mode takes on added importance. Once an algorithm and methodology is verified with simulated data, then the same approach could be applied to CryoSat data, over a wide variety of oceanic or inland water conditions. The results should have considerable value beyond the lifetime of the SAMOSA project itself.

**Comments on specific algorithms**

Several high-level “lessons learned” follow from the investigations reported in this technical note:

**On pre-summing**. The initial approach (Version 1), which was motivated by an effort to conserve (additive) SNR, led to peaked waveforms quite unlike the intended LRM Brown-model waveforms. This peakedness is a consequence of the pulse-to-pulse correlation produced by the pulse-limited area on the (simulated) surface. As such, it provides an indirect confirmation of the fidelity of the CRYMPS simulation of the details of oceanic backscatter. However, the lesson learned is that the SAR-mode-to-pseudo-LRM transformation algorithm should not use presuming, or any form of coherent pulse-to-pulse combination for that matter. That conclusion is implicit in the upper bound on radar pulse-repetition frequency (PRF), the incoherent limit described by Walsh (1982).

**Doppler selection**. An alternative to pre-summing is to take the Fourier transform of the data in azimuth, across the data at a constant range over each burst, in the same way that opens the delay-Doppler algorithm. This would redistribute the samples by Doppler bin, which correspond to spacing at the surface of about 250 meters. Since the resulting waveforms reside in disjoint (Doppler) frequency bands, they would be statistically independent. However, one consequence of Doppler binning is to change the shape of the resolved backscatter area to be Doppler delimited along track and pulse-limited across track. The result? A peaked waveform, in this instance because of the asymmetrical footprint, rather than pulse-to-pulse correlation. Hence, along-track Doppler decomposition must be avoided in this context. Of course, an along-track FFT when viewed in the abstract is a form of “coherent summing”, and so should be ruled out by application of the principle above.

**Waveform selection**. Within a given SAR-mode burst, the PRF is higher than that of the LRM mode by approximately a factor of 9. Thus, consider a sub-set of pulses comprised of every ninth pulse within a SAR-mode burst. The resulting waveforms approximate closely their counterparts in the LRM mode, especially with respect to pulse-to-pulse correlation. The general lesson learned here is that taken individually, none of the waveforms “know” that they are part of a SAR-mode sequence, as opposed to an LRM sequence. It follows that a subset of waveforms so selected from a SAR-mode burst (at least for that subset) represents the closest possible imitation of LRM mode data that the SAR-mode data conveys.

**Statistics and degrees-of-freedom**. Given that waveforms are selected carefully within the confines of each burst, and at a rate comparable to the LRM PRF, between bursts there are no waveforms available from the SAR mode. This is in contrast to the LRM mode, in which waveforms occur regularly regardless of where the SAR bursts may be. Measurement statistics in general—and variance in particular—depend intimately on the number of independent waveforms that are averaged (incoherently summed). Thus, if the two modes are to be compared based on SAR-mode-derived waveforms, then the discrepancy in the number of independent waveforms has to be accounted for. A method that respects this constraint is described in the recommendations.

# 11. CONCLUSIONS & RECOMMENDATIONS

A study of the improvement in range and SWH retrieval performance of SAR altimeters compared to pulse-limited altimeters in different SWH conditions was attempted, based on simulated LRM and SAR products from the CRYMPS simulator for a number of open waters scenarios. The sampling and averaging of the CRYMPS SAR burst data into pseudo-LRM waveforms were performed with the RDSAR software.

Two versions of the CRYMPS runs and of the RDSAR software were assessed in this study. In neither case was it possible to compute the final results on range error versus SWH. The reasons are as follows:

1) RDSAR_v1 led to excessively peaky RDSAR waveforms, linked to uncertainties about the correct methodology to perform coherent and incoherent averaging

2) RDSAR_v3 led to excessively noisy RDSAR waveforms, linked to the much smaller (32) number of waveforms averaged when using incoherent averaging only. Simply “scaling the retrieved range error” by sqrt(N) to answer the original question (improved performance of DDA v pulse-limited) is not tenable since increasing the number of waveforms implies coherent averaging which follows different statistics.

3) Significant delays and considerable additional work resulted from the use of an inappropriate and sensitive ice tracker in CRYMPS applied to the case of open ocean scenarios. This generated artefacts in the CRYMPS products, which necessitated repeats of all runs and analyses.

4) Along-track shift and excessive noisiness of the retrieved SWH in RDSAR_v3 products makes it difficult to identify precisely the data segments relevant to particular SWH conditions.

Our **specific recommendations** to take this work forward are as follows:

1) To perform a rigorous assessment of the CRYMPS SAR products by examining the statistics of CRYMPS SAR waveforms against LRM. This could be done by comparison with theory or with another numerical CryoSat simulator.

2) To perform a comprehensive study to determine the best sampling and averaging strategy to reduce SAR burst data to pseudo-LRM waveforms while preserving the noise-reducing capability linked to the larger number of waveforms in SAR mode.

3) To provide access to a form of the RDSAR software tool to enable free and flexible investigations of DDA SAR products, of different sampling/averaging strategies and the implications for range retrieval. This could be either through access to the RDSAR source code or to a modified version of the RDSAR software where sampling and averaging are customisable by the user.

4) To modify the RDSAR product to preserve the along-track time and/or latitude/longitude information present in the CRYMPS SAR products.

**General recommendations**

**On time of observation**. As is well known, measurement variance is reduced as the degrees-of-freedom in the measurement is increased. Thus, if the objective is to establish the relative difference in measurement precision between modes, then the basis for comparison must span as large a number of pulses as is reasonably possible, rather than being confined to a short basis, such as 1/20 of one second. Second, as long as the underlying surface features are (statistically) invariant, then it does not matter how long the (simulated or real) observation lasts. Thus, to increase the confidence in any estimate of the difference in measurement variance between the two modes, the averaging time should be as long as possible. At the outset, this will be limited by the length of CRYMPS runs (less potential end effects, if any). As a corollary, the primary comparison should be based on measurement precision, and the statistics of shorter averaging times (or of the mode's response to a change in sea-state) should take second priority.

**CRYMPS qualification**: the control experiment. Regardless of the algorithm employed to derive pseudo-LRM waveforms from SAR-mode waveforms, there must be a test to verify that the method is reliable. In principle, the candidate algorithm should be applied to SAR-mode data for a given input scenario, for which there also exist LRM waveforms. Then the test is comprised of quantitative comparisons of the pseudo-LRM measurements with the LRM measurements. These tests must demonstrate statistical equivalence. Any SAR-mode-to-pseudo-LRM mode transformation algorithm must pass this test before the pseudo-LRM data that it generates can be qualified for use in further experiments and comparisons.

A simple method to generate pseudo-LRM data is comprised of four steps: (1) run CRYMPS once over a constant sea-state scenario (to generate simultaneous SAR mode and LRM mode waveforms); (2) choose n seconds of contiguous LRM waveforms, resulting in a group of n x PRF LRM waveforms; (3) select n x PRF LRM waveforms from the SAR-mode bursts (noting that this will require a sequence of SAR-mode data nearly 3 times longer in order to gather exactly the same number of waveforms as in the LRM group); and (4) compare the statistics of the two groups. Such a control experiment gets data in the “true-LRM” mode and from the “pseudo-LRM” mode that should be statistically identical. The averaging time should be as large as possible in order to expose small differences in the variances of the results.

For example, if the intended interval is one second (n=1), then the LRM mode data would have 1970 waveforms. The pseudo-LRM data would require the underlying SAR mode sequence to last nearly three seconds to supply an equal number of waveforms. Eight waveforms should be selected from each SAR-mode burst, one waveform of every 9. This should be repeated for about 250 bursts, to accumulate 1970 waveforms. The essential points are (i) that the same number of waveforms be assembled for both modes, and (ii) during a burst interval that the same PRF be replicated (as closely as the burst mode allows). In principle, the two sets of waveforms (square-law detected and compressed) from the LRM run and the SAR-mode run should be statistically identical. If this proves to be true, then CRYMPS SAR-mode individual waveforms can be accepted with confidence to be the statistical equivalent to individual waveforms from the LRM mode. If not true, then CRYMPS would have to be enhanced to pass this or any similar test before its data could be used as intended for WP2. (Note: Variations on this validation experiment include proportionally reducing the length of the two runs if required, and running the same procedure over two or more SWH scenarios.)

**Quantitative comparison of modes:** the validation experiment. Once confidence is established in the transformation of SAR-mode data into pseudo-LRM data that is statistically equivalent to “true” LRM data, then SAR-mode data (either from CRYMPS or CryoSat) are sufficient to set up experiments to investigate the relative performance of the two modes under a variety of sea-state conditions. The method is loosely patterned after the design of the control experiment. To summarize, a validation experiment is comprised of three steps: (1) select individual waveforms from SAR-mode data (as described above) of duration approximately three times as long as the intended averaging time n seconds to assemble the pseudo-LRM group; (2) select the corresponding SAR-mode data of duration n seconds; (3) calculate the desired statistics on the two groups each representing n seconds of observation in their respective modes, and compare. Note that the basis for comparison must be the same equivalent observation (averaging) time n seconds for both, since that is the only fair way to compare their performance. Of course, it takes a longer time to assemble the pseudo-LRM data group, but that is irrelevant to the comparison, which must be faithful to the statistics, especially regarding the “degrees-of-freedom” of the two types of measurement, per unit time.

**Trade-offs**. Since the SAR mode and the LRM mode PRF patterns are so different, some compromise in the experiment boundary conditions has to be accepted before the resulting “true” and “pseudo” LRM waveforms can be expected to converge to statistical similarity. Candidate parameters for trade include, for example, adjusting the variances to account for any difference in the number of independent waveforms summed in each case, or crafting “filler waveforms” to stand in for the missing ones. Other compromises include the strategy outlined above, namely, the use of pseudo-LRM waveforms selected from a longer duration of the SAR-mode data so that when the two modes are compared statistically, they correspond to the correct number of pulses in each case that would be observed in a given time interval. All such schemes imply advantages as well as disadvantages. The trade-off should favour the most reliable result with the least affront to the underlying physics. The method outlined above is recommended, based in part on the experience gained to date on SAMOSA.

**Waveform posting rate.** The project should give serious consideration to expanding the nominal period of comparison from 1/20 second to as long as the simulation can support. Given that the objective is to compare the intrinsic precision of two different radar altimeter architectures, rate of waveform posting is irrelevant. If shorter posting intervals are of interest, then the resulting variances of a longer observation time can be scaled (by the square root of the time ratio) to a shorter time. Scaling to shorter time intervals from long is far more robust than attempting to scale short-time variances to long-term measurements.

**Observation times.** There is no fundamental requirement that the data collection time for the waveforms required to assemble the pseudo-LRM data must equal the intended averaging time for the end comparisons. Indeed, this degree of freedom is the least risky of those that one might consider when trying to bring the statistics of the two modes into convergence. Set up the input scenarios so that the dwell time in each sea state is sufficiently long that the SAR-mode data will have enough time to accumulate an equivalent number of statistically independent waveforms in the pseudo-LRM mode as an equivalent LRM mode. It is worth noting that this method should apply equally well to actual CryoSat data.

**Waveform accommodation**. SAR-mode waveforms are peaked, in contrast to the conventional “Brown-model” LRM waveforms. Comparison between these two types requires compatible retracking and parameter estimation algorithms. Jensen (J. R. Jensen, "Radar altimeter gate tracking: theory and extension," IEEE Transactions Geoscience and Remote Sensing, vol. 37, pp. 651-658, 1999) derived an algorithm that transforms SAR-mode (delay-Doppler) waveforms into conventional waveforms. The project should consider adopting the Jensen transformation (or an equivalent operator) so that the measurement precision ascribed to data from the two modes may be compared reliably.

## 12 - REFERENCES

Cullen, R.A. & Wingham, D.J., 2002: CryoSat Level 1b processing algorithms and simulations results, IGARSS’02.

Francis, C. R. et al., 2007: CryoSat Mission and Data description, CS-RP-ESA-SY-0059, Jan. 2007

Gommenginger, C.P., P. Cipollini, C. Martin-Puig, J. Marquez, P. D. Cotton, R. K. Raney & J. Benveniste, SAR Altimetry numerical simulations over water surfaces, EGU General Assembly 2008, Vienna, 13-18 April 2008.

Jensen & Raney, 1998. Delay Doppler radar altimeter: Better measurement precision. Proceedings IEEE Geoscience and Remote Sensing Symposium IGARSS'98. Seattle, WA, IEEE**:** 2011-2013.

Martin-Puig, C., J. Marquez, G. Ruffini, G., R. K Raney & J. Benveniste, SAR ALTIMETRY APPLICATIONS OVER WATER, SeaSAR'2008, 2008a.

Martin-Puig, C., et al., SAMOSA RDSAR User Manual, 2008b.

Martin-Puig, C., et al., SAMOSA Reduced SAR Mode Software Requirements Document (SRD), 2008c.

Martin-Puig, C., et al., SAMOSA Reduced SAR Mode Software Design Document (SDD), 2008d.

## ANNEX 1: RV1 RESULTS

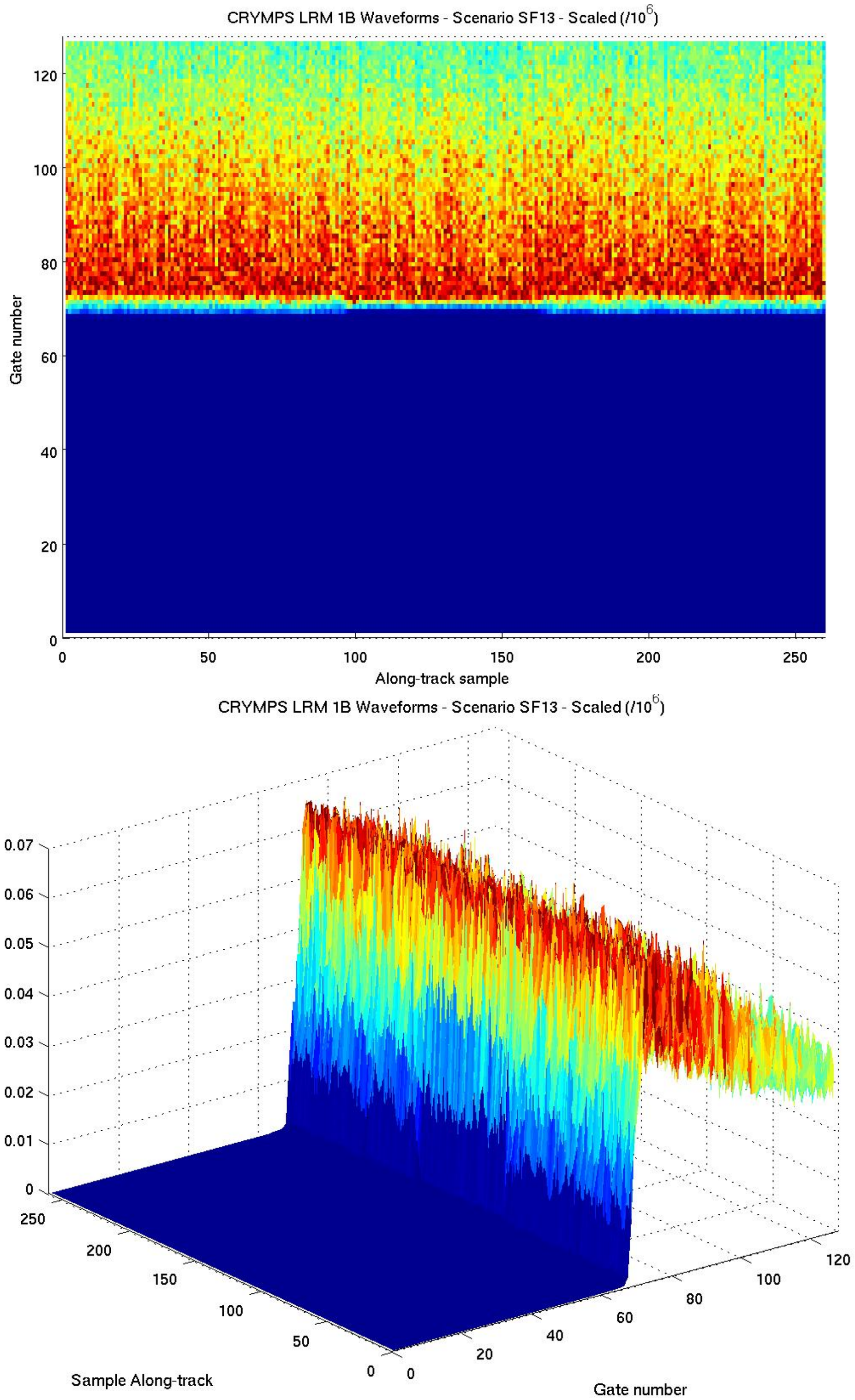


***Figure 25 – CRYMPS Low-Resolution Mode (LRM) waveforms for open ocean scenario SF13 (RV1)***

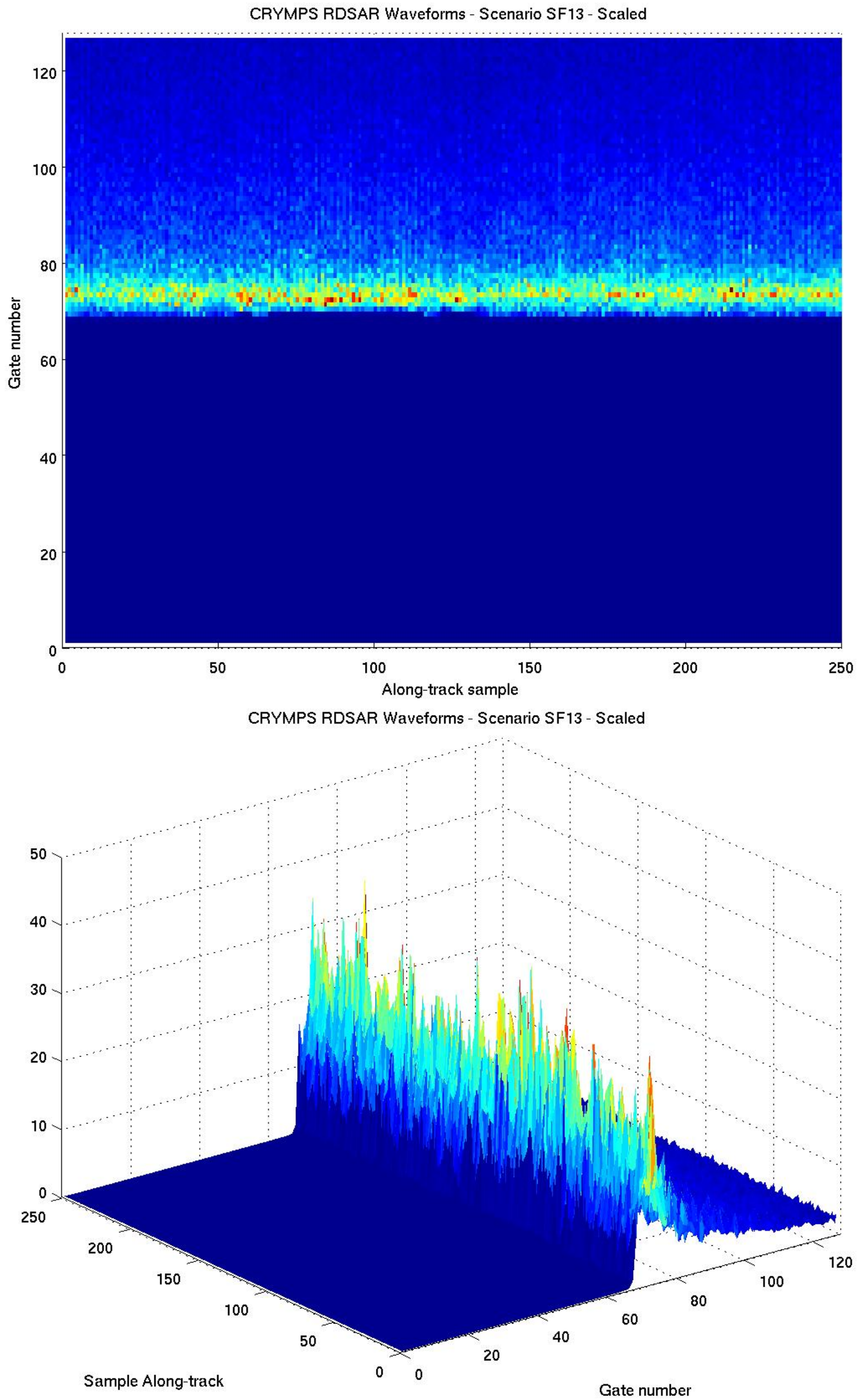


***Figure 26 – CRYMPS Reduced SAR (RDSAR) waveforms for open ocean scenario SF13 (RV1)***

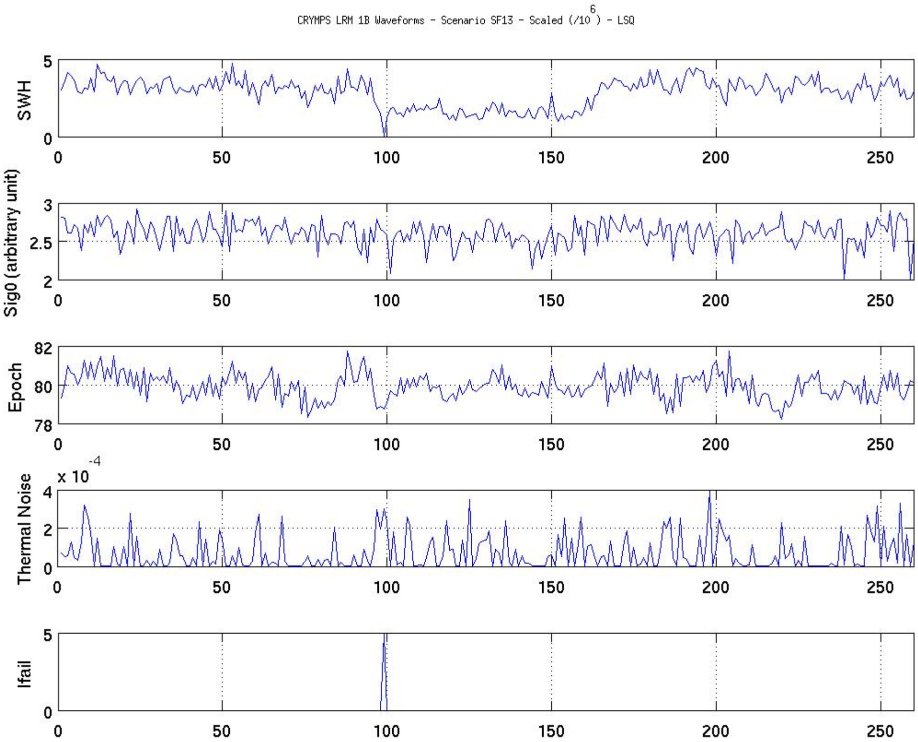


***Figure 27 – NOCS ocean retracker (top to bottom) retrieved SWH, Sigma0, epoch, thermal noise and retrieval quality flag for CRYMPS LRM waveforms (scaled by 106) for scenario SF13 (RV1)***

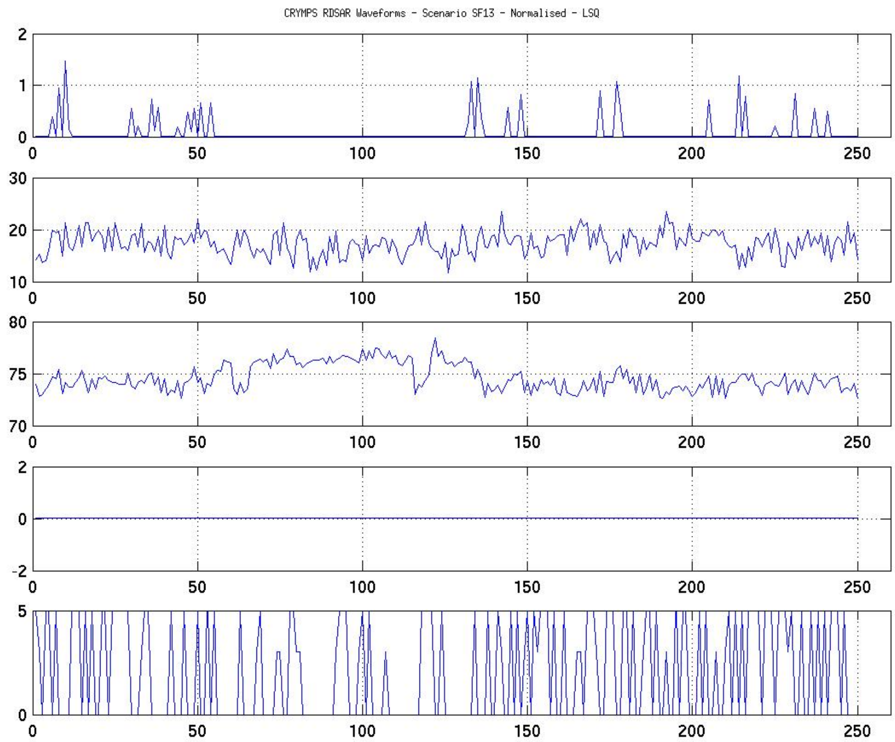


***Figure 28 – NOCS ocean retracker (top to bottom) retrieved SWH, Sigma0, epoch, thermal noise and retrieval quality flag for CRYMPS RDSAR waveforms (normalised) for open ocean scenario SF13 (RV1).***

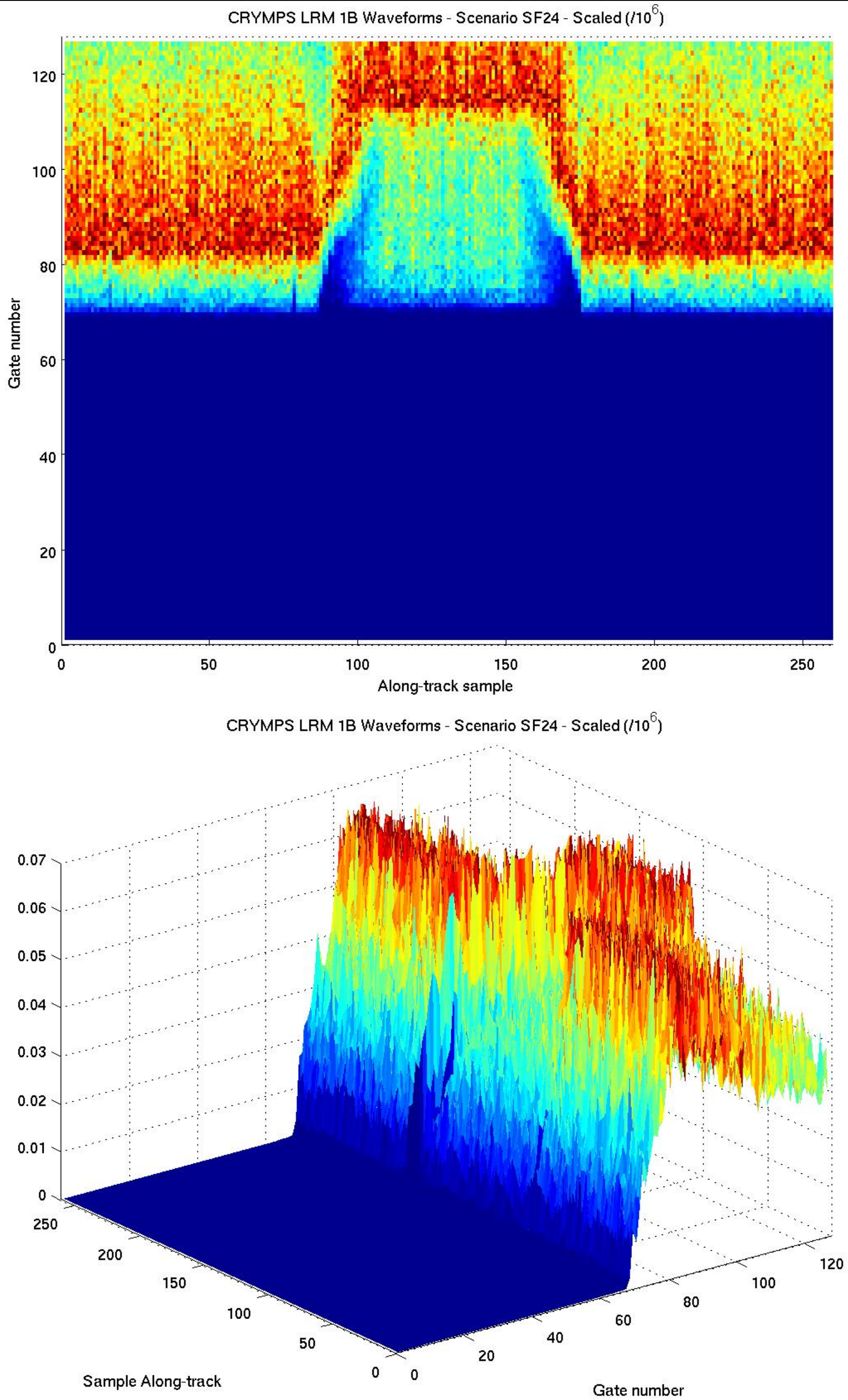


***Figure 29 – CRYMPS Low-Resolution Mode (LRM) waveforms for open ocean scenario SF24 (RV1)***

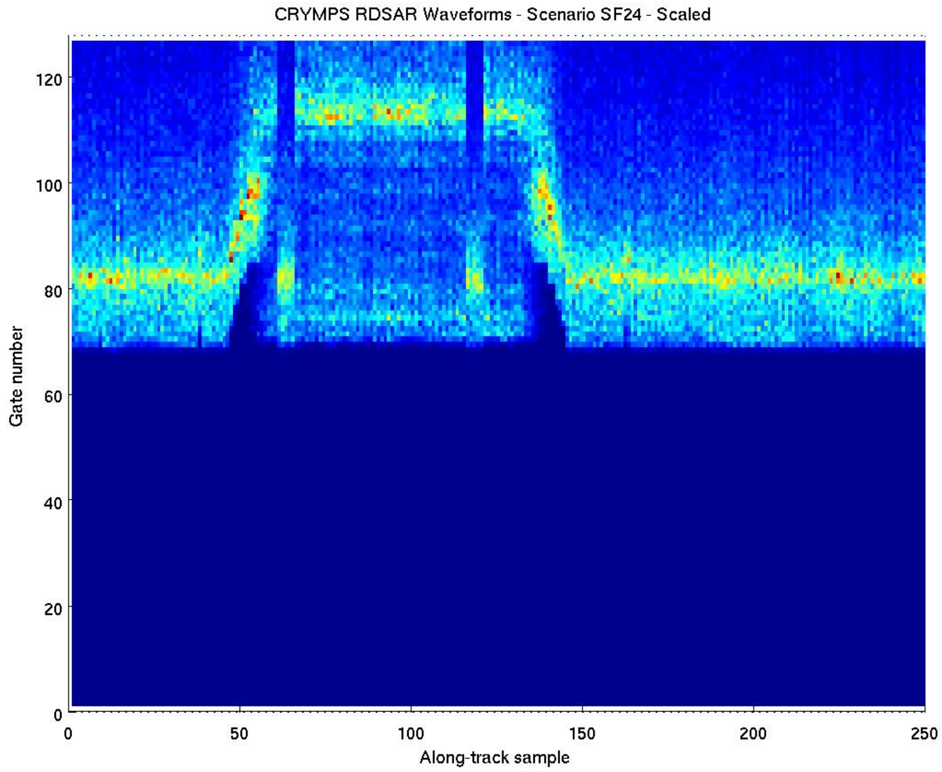


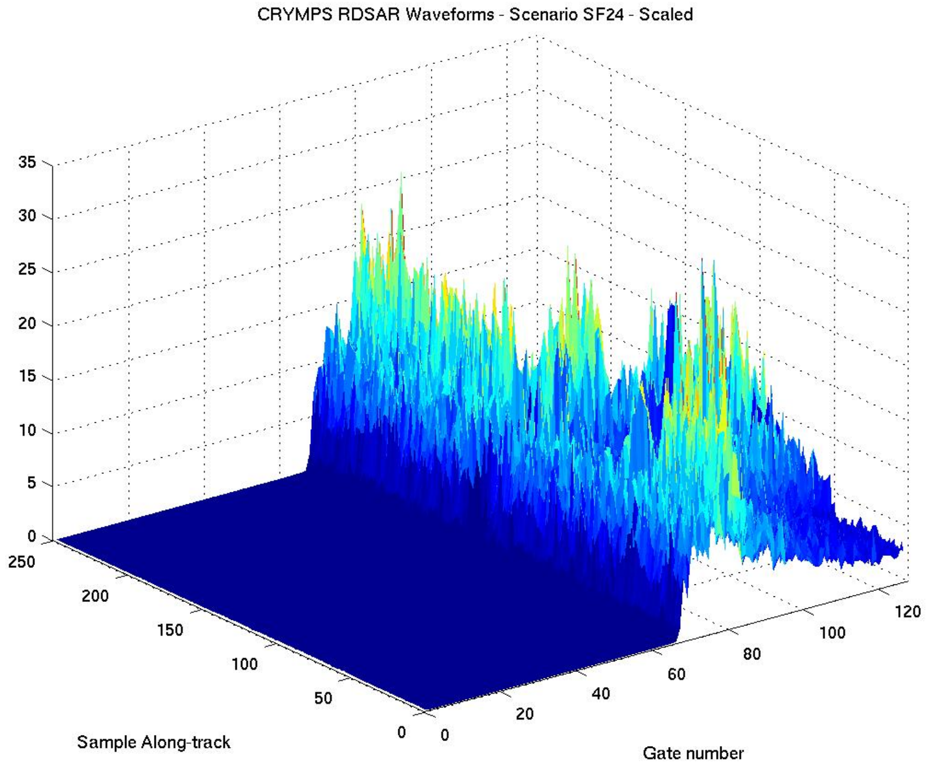


***Figure 30 – CRYMPS Reduced SAR (RDSAR) waveforms for open ocean scenario SF24 (RV1)***

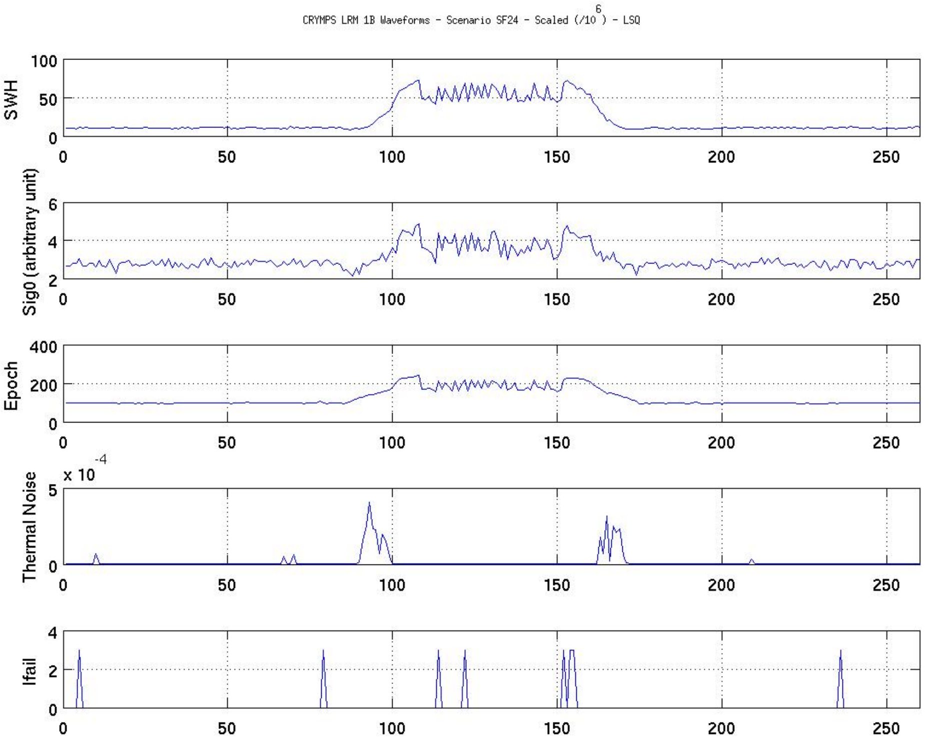


***Figure 31 – NOCS ocean retracker (top to bottom) retrieved SWH, Sigma0, epoch, thermal noise and retrieval quality flag for CRYMPS LRM waveforms (scaled by 106) for open ocean scenario SF24 (RV1).***

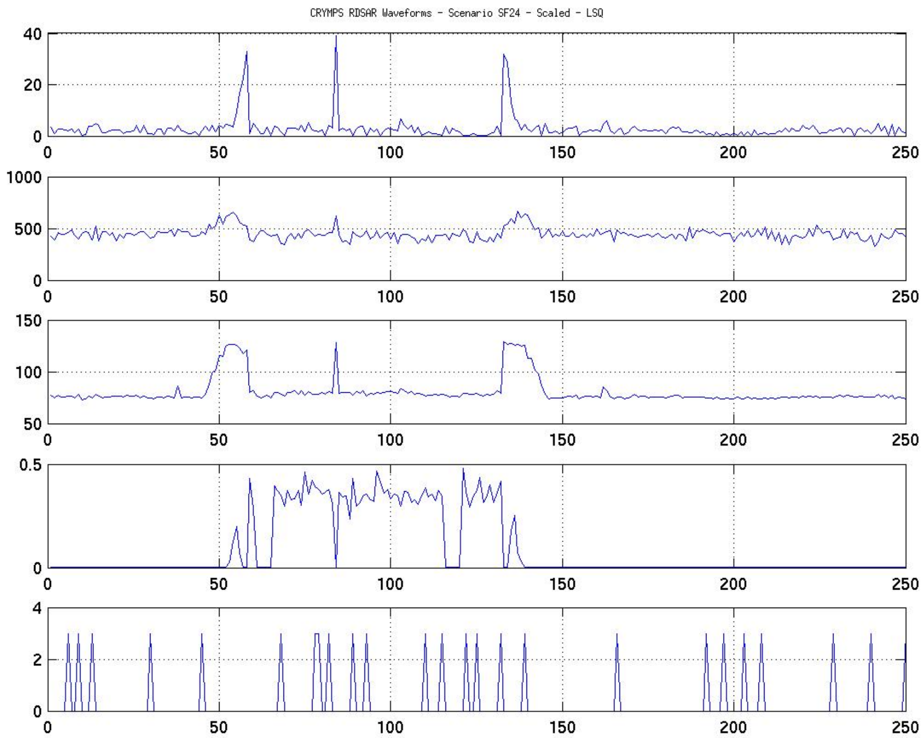


***Figure 32 – NOCS ocean retracker (top to bottom) retrieved SWH, Sigma0, epoch, thermal noise and retrieval quality flag for CRYMPS RDSAR waveforms (scaled by 1, i.e. unscaled) for open ocean scenario SF24 (RV1).***

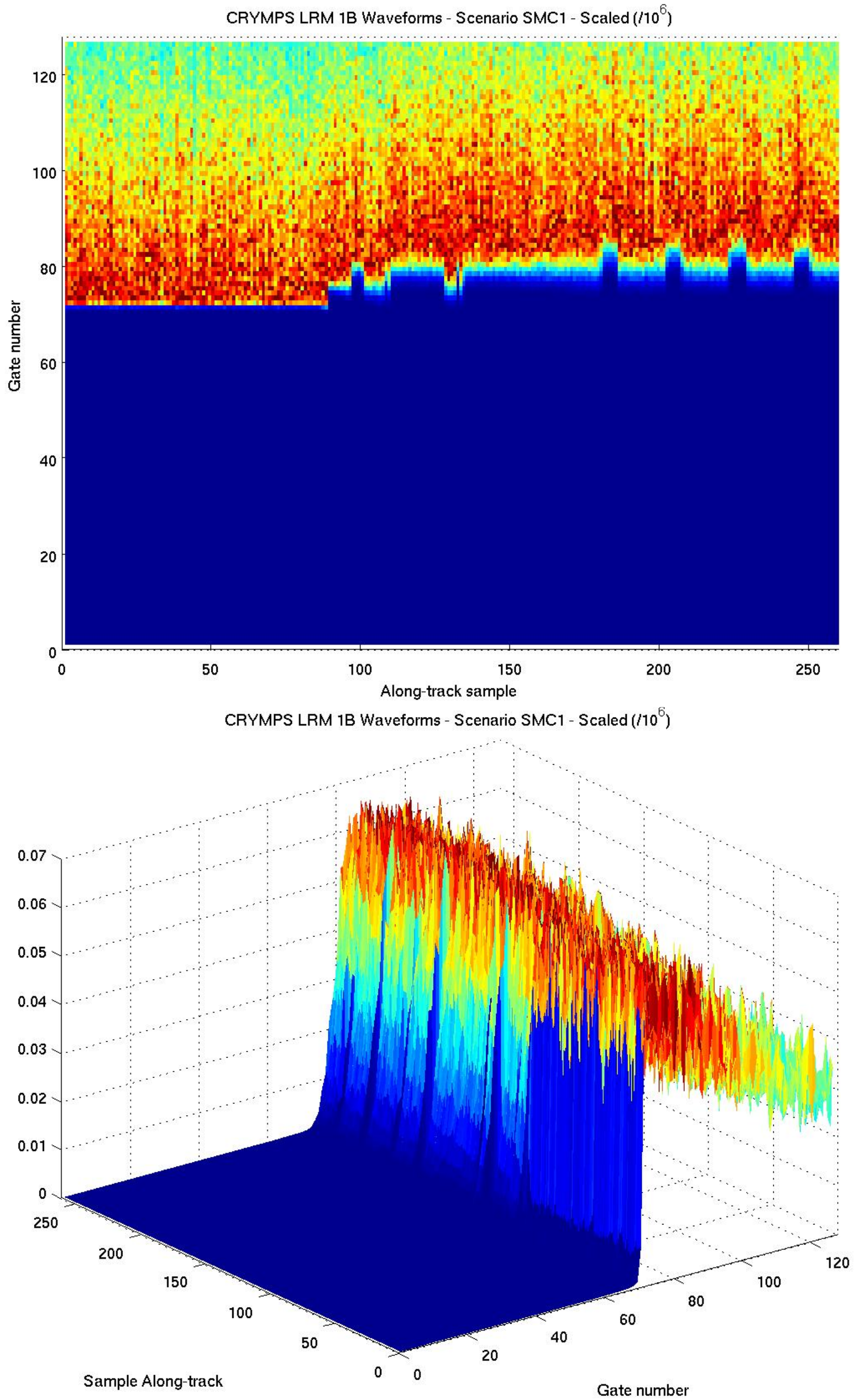


***Figure 33 – CRYMPS Low-Resolution Mode (LRM) waveforms for open ocean scenario SMC1 (RV1)***

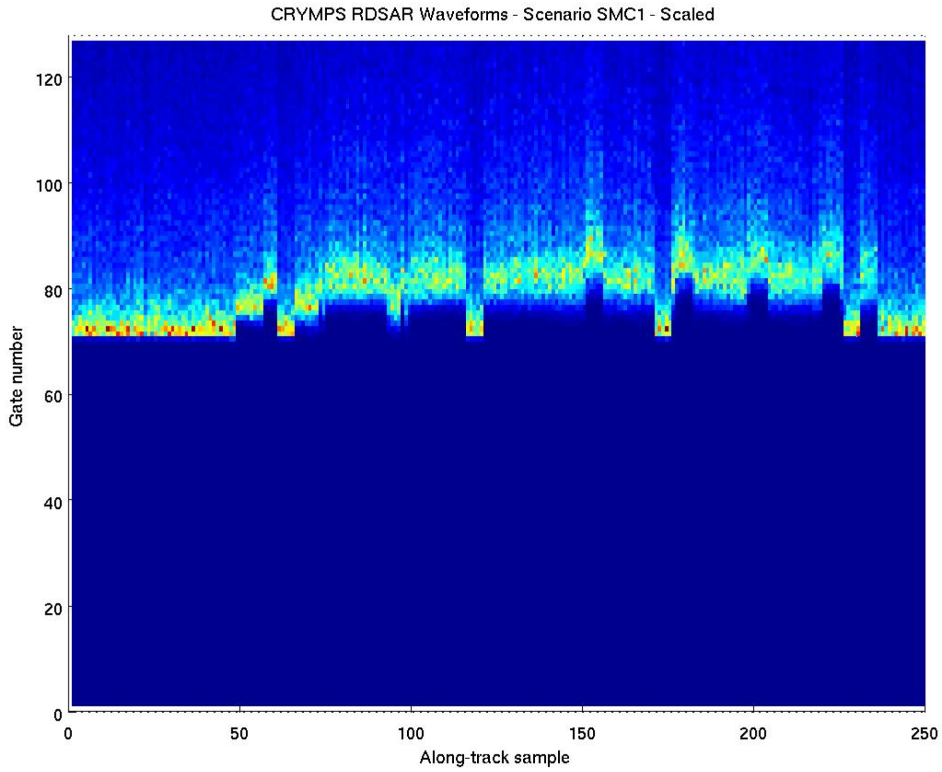


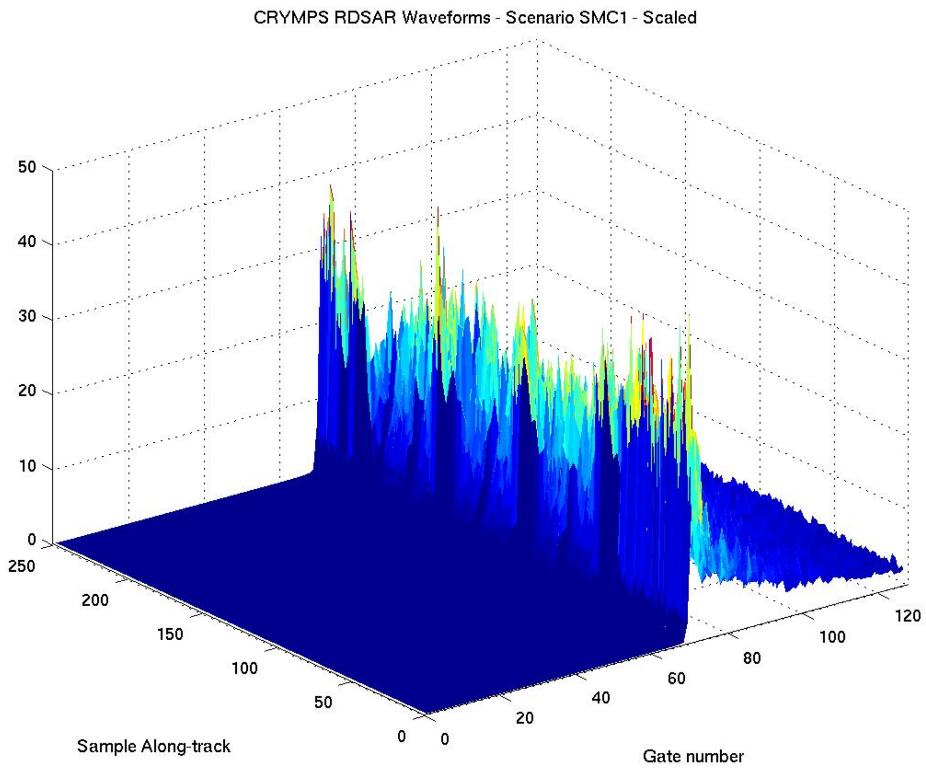


***Figure 34 – CRYMPS Reduced SAR (RDSAR) waveforms for open ocean scenario SMC1 (RV1)***

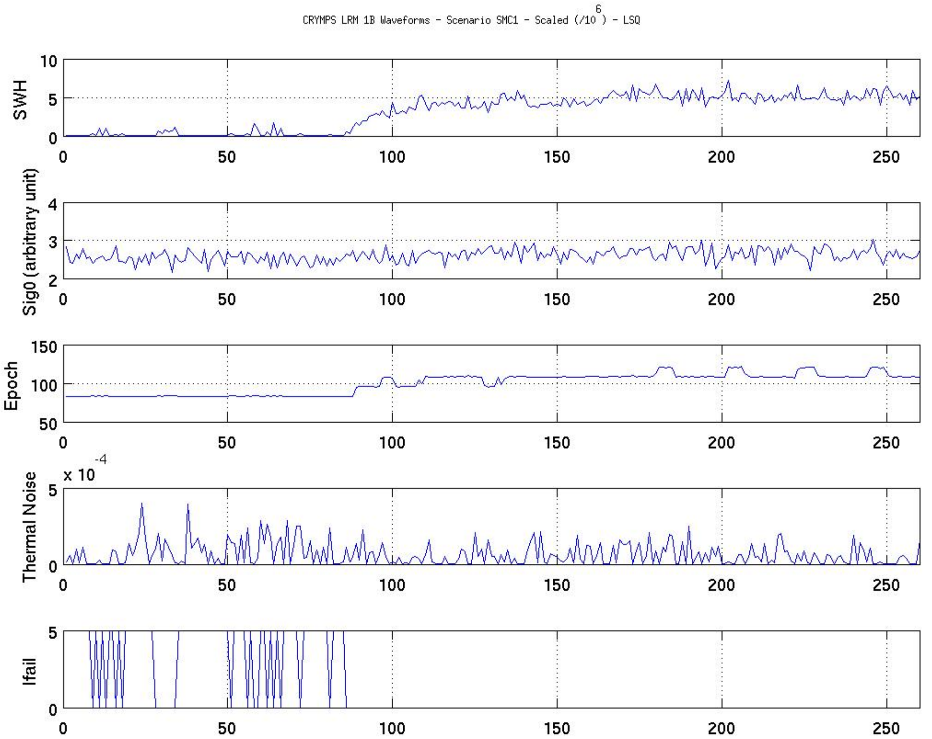


***Figure 35 – NOCS ocean retracker (top to bottom) retrieved SWH, Sigma0, epoch, thermal noise and retrieval quality flag for CRYMPS LRM waveforms (scaled by 106) for open ocean scenario SMC1 (RV1).***

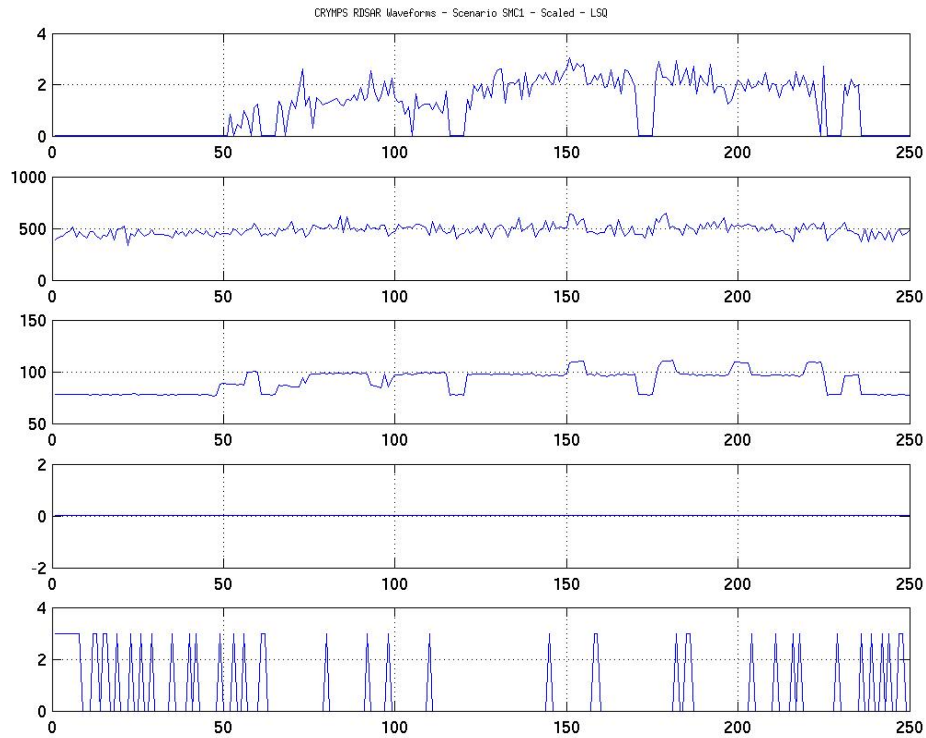


***Figure 36 – NOCS ocean retracker (top to bottom) retrieved SWH, Sigma0, epoch, thermal noise and retrieval quality flag for CRYMPS RDSAR waveforms (scaled by 1, i.e. unscaled) for open ocean scenario SMC1 (RV1).***

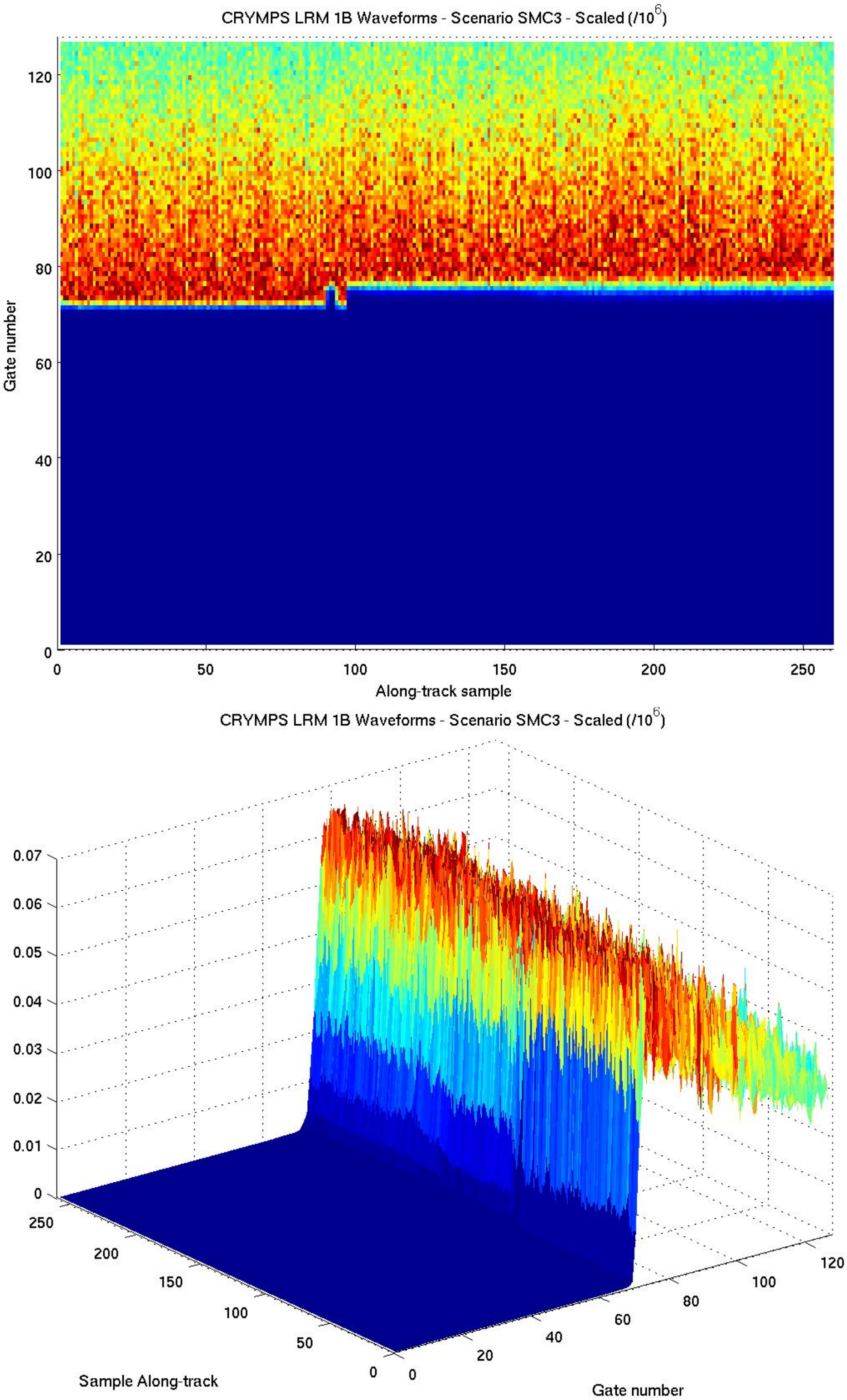


***Figure 37 – CRYMPS Low-Resolution Mode (LRM) waveforms for open ocean scenario SMC3 (RV1)***

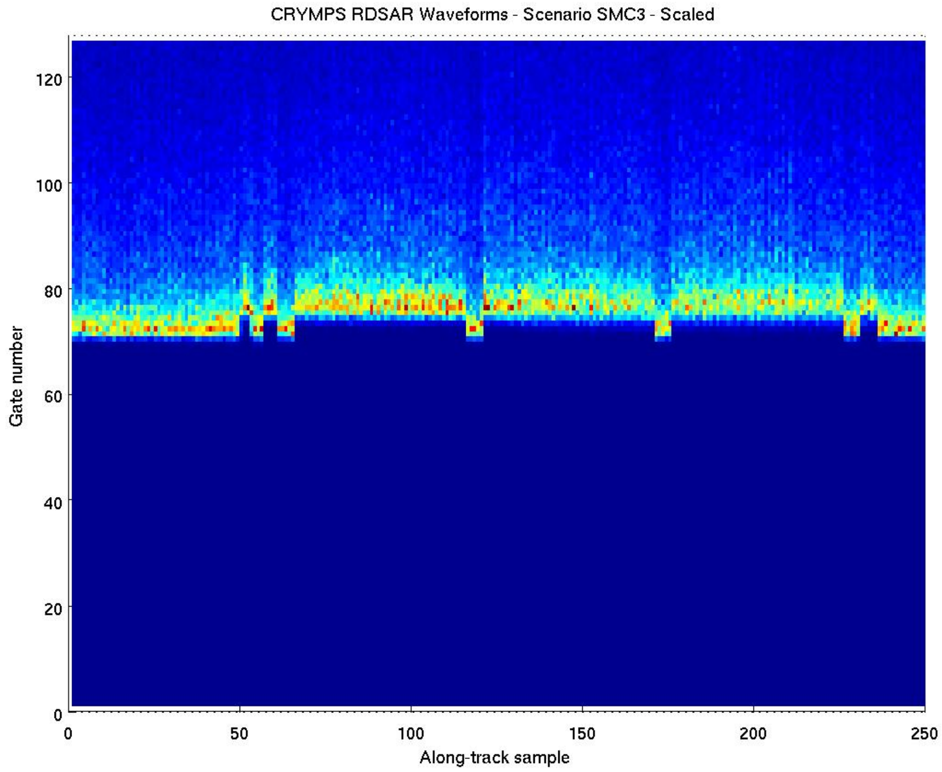


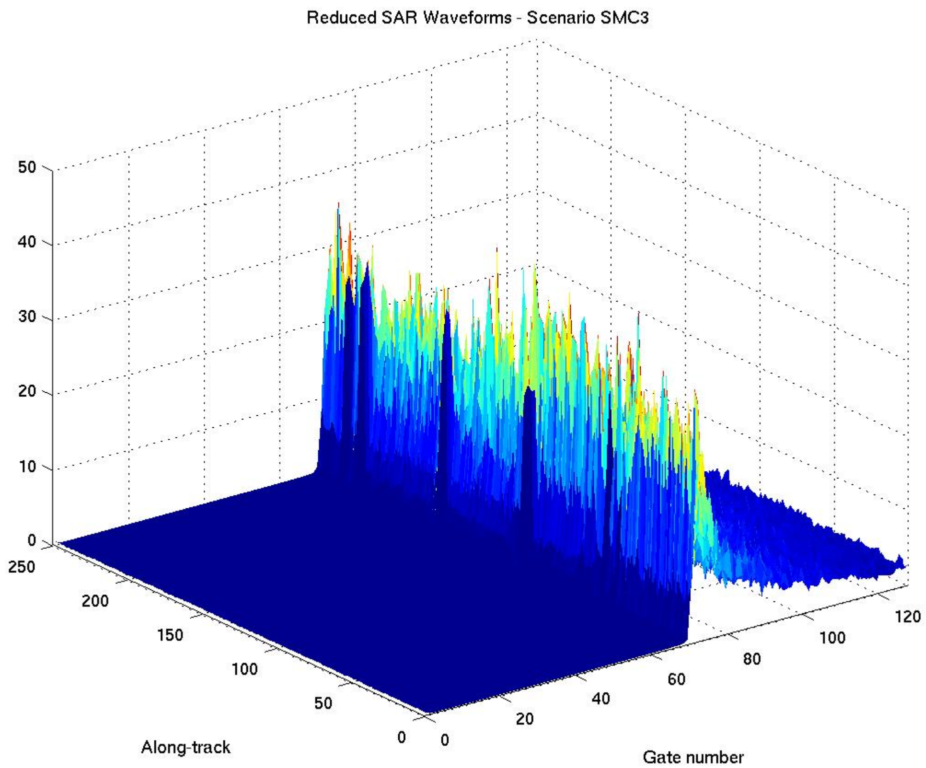


***Figure 38 – CRYMPS Reduced SAR (RDSAR) waveforms for open ocean scenario SMC3 (RV1)***

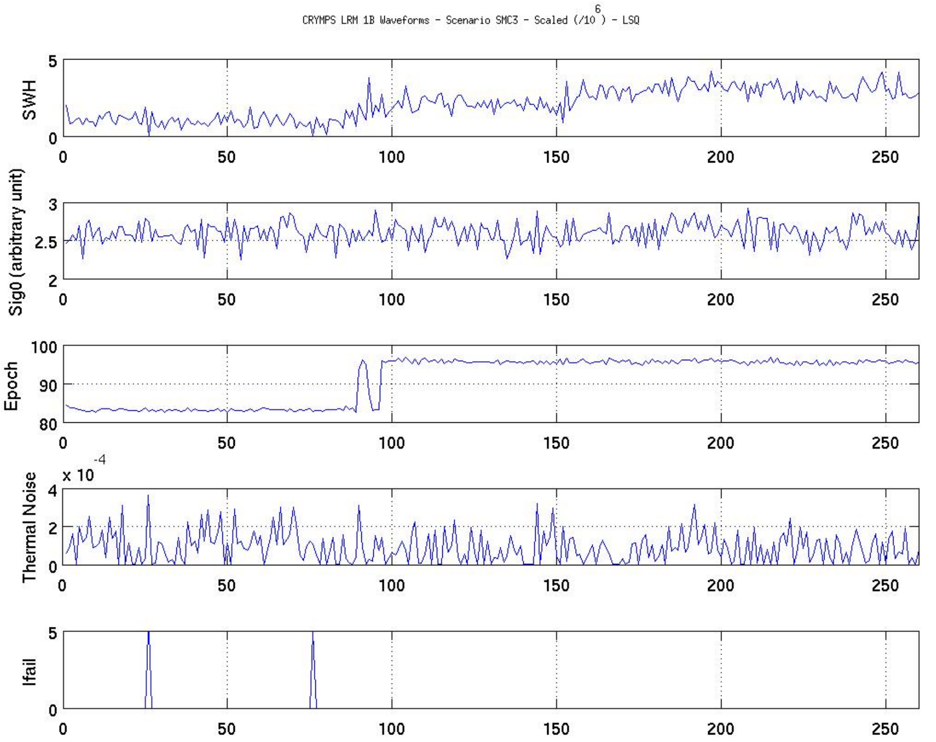


***Figure 39 – NOCS ocean retracker (top to bottom) retrieved SWH, Sigma0, epoch, thermal noise and retrieval quality flag for CRYMPS LRM waveforms (scaled by 106) for open ocean scenario SMC3 (RV1).***

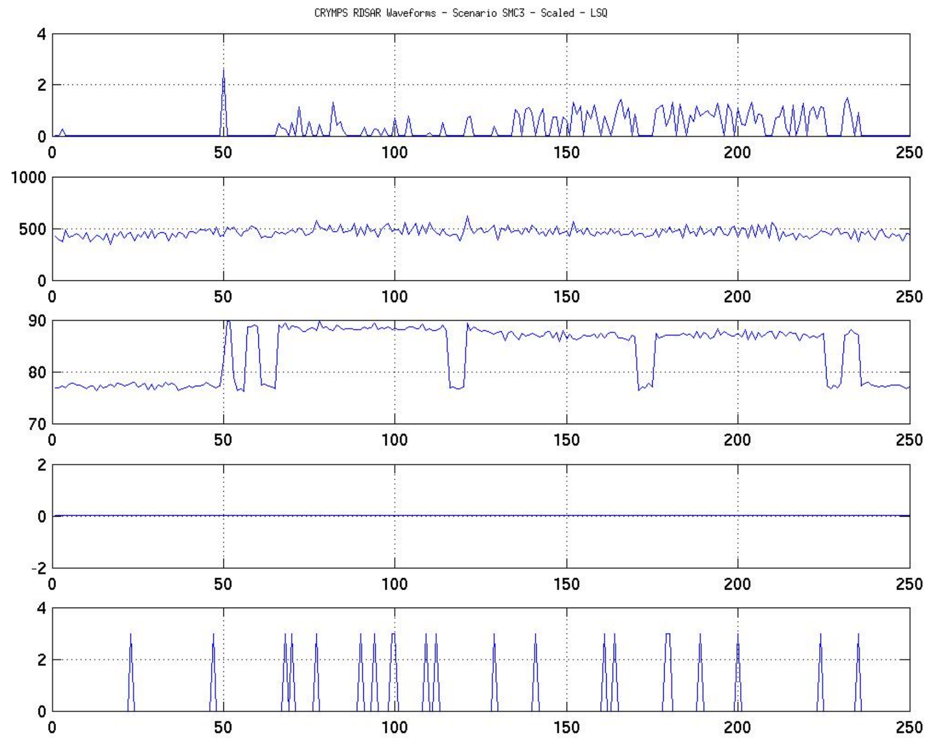


***Figure 40 – NOCS ocean retracker (top to bottom) retrieved SWH, Sigma0, epoch, thermal noise and retrieval quality flag for CRYMPS RDSAR waveforms (scaled by 1, i.e. unscaled) for open ocean scenario SMC3 (RV1).***

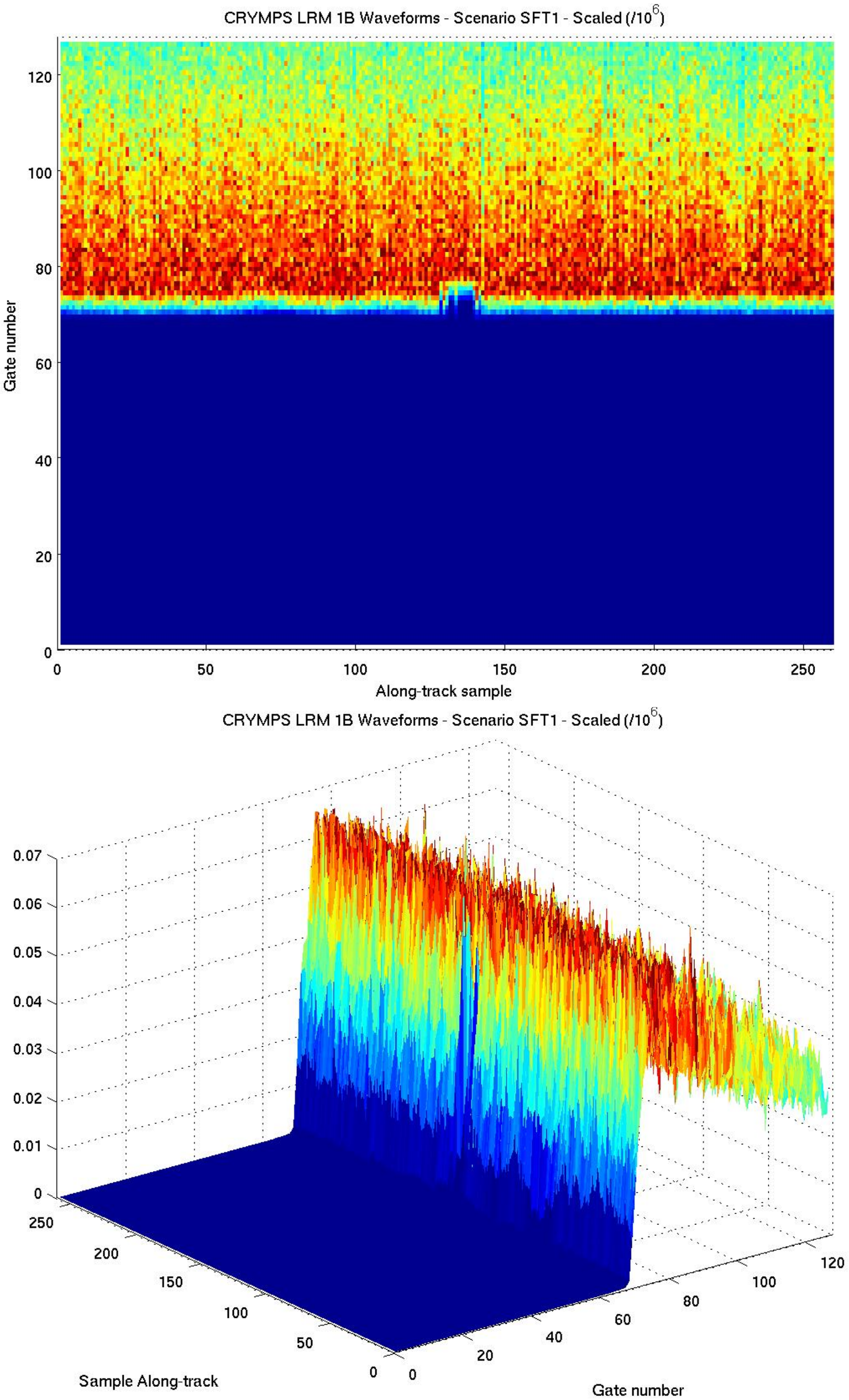


***Figure 41 – CRYMPS Low-Resolution Mode (LRM) waveforms for open ocean with bathymetry scenario SFT1 (RV1)***

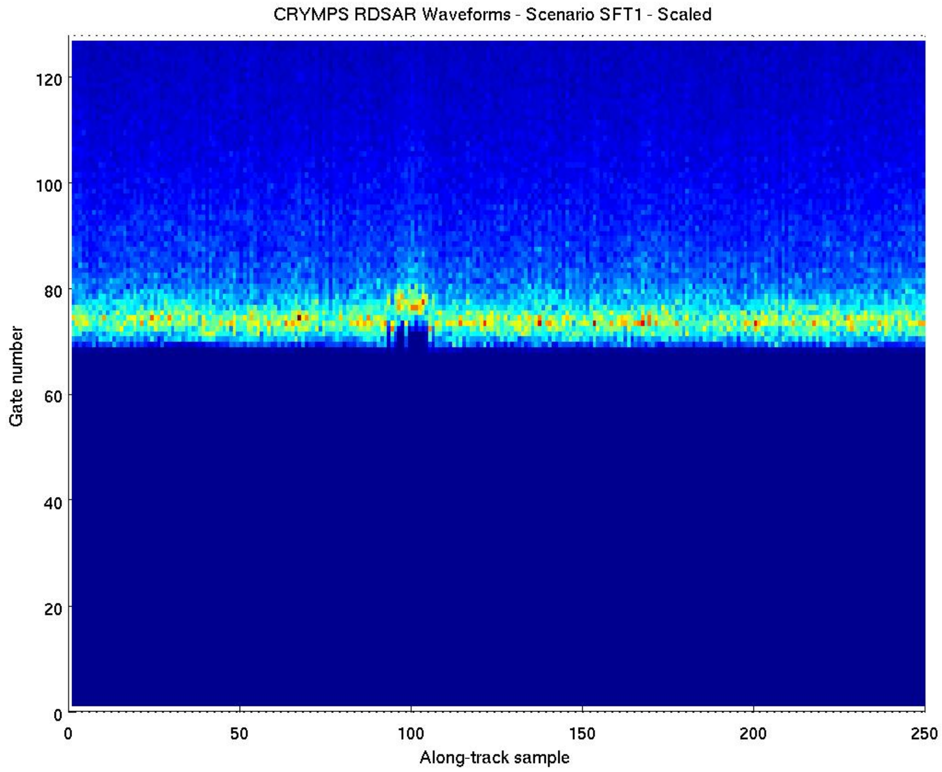


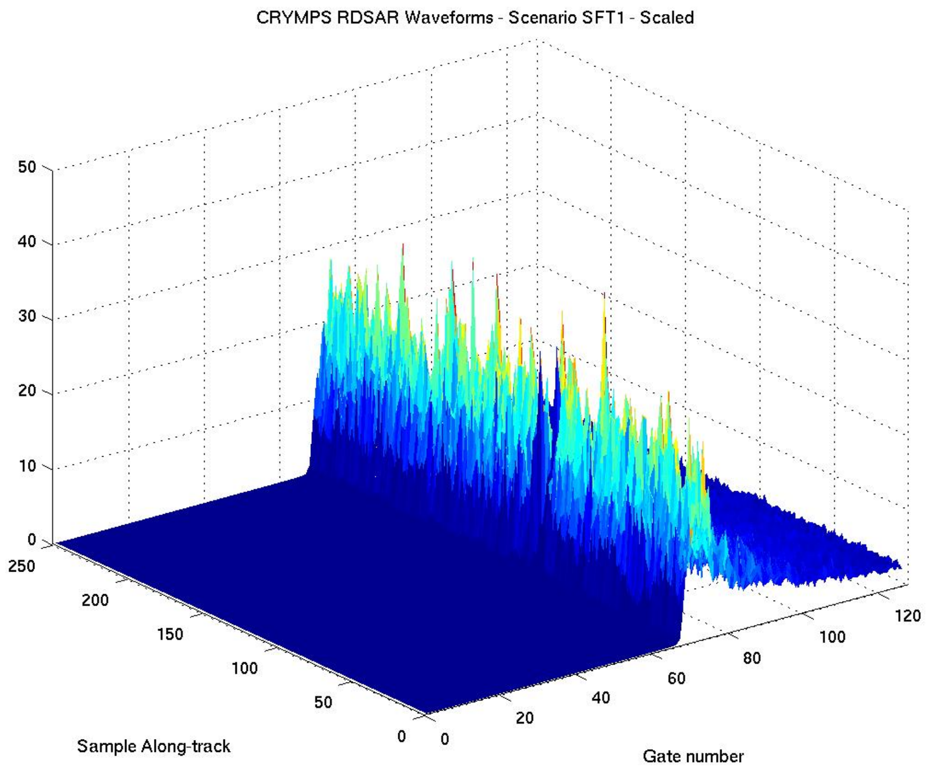


***Figure 42 – CRYMPS Reduced SAR (RDSAR) waveforms for open ocean with bathymetry scenario SFT1 (RV1)***

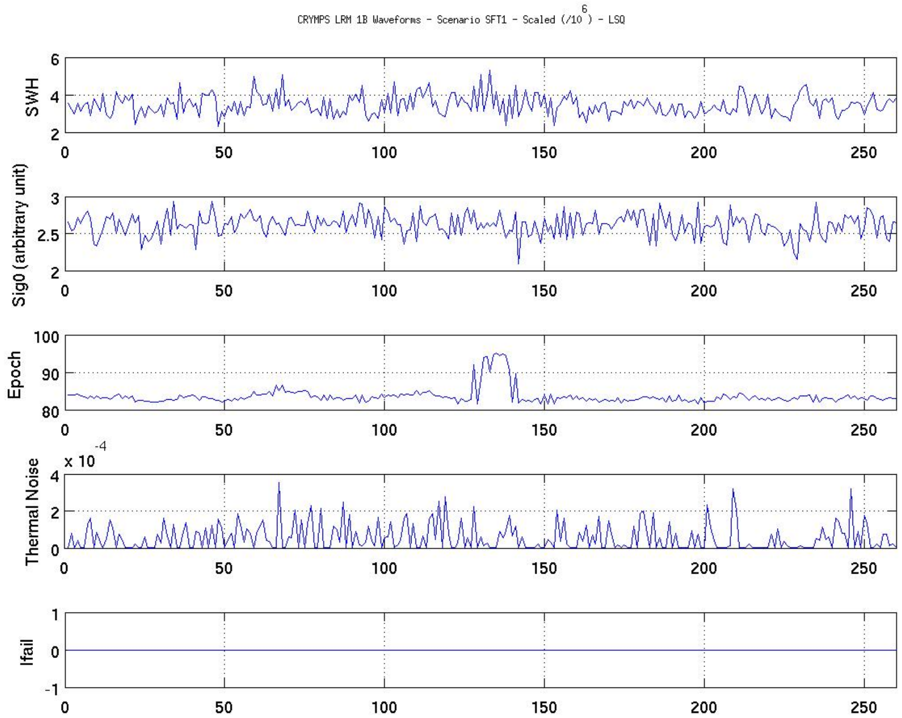


***Figure 43 – NOCS ocean retracker (top to bottom) retrieved SWH, Sigma0, epoch, thermal noise and retrieval quality flag for CRYMPS LRM waveforms (scaled by 106) for open ocean scenario SFT1 (RV1).***

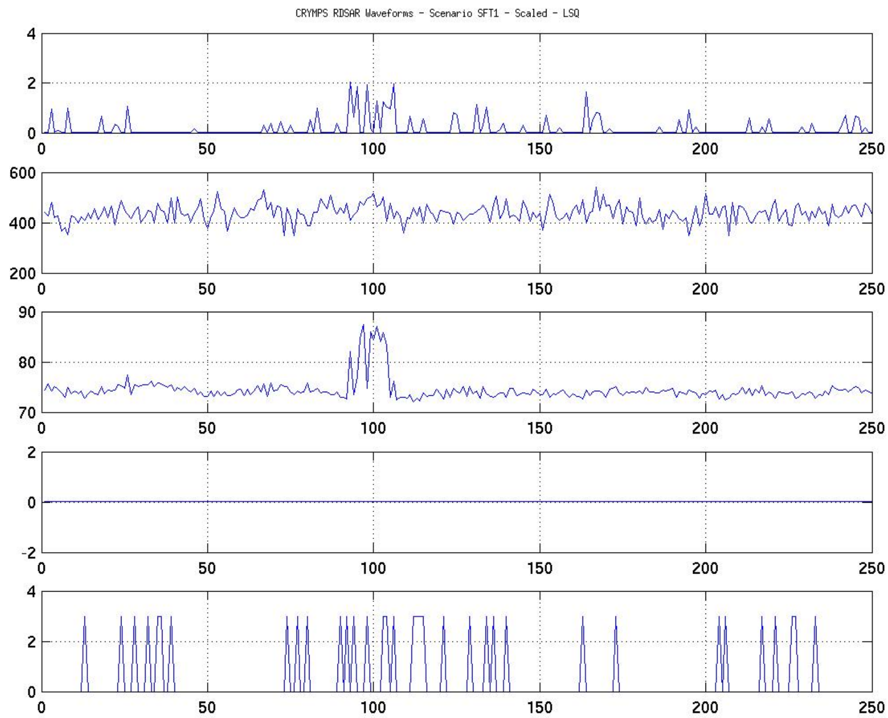


***Figure 44 – NOCS ocean retracker (top to bottom) retrieved SWH, Sigma0, epoch, thermal noise and retrieval quality flag for CRYMPS RDSAR waveforms (scaled by 1, i.e. unscaled) for open ocean scenario SFT1 (RV1).***

## ANNEX 2: DETAIL OF INTERNAL PROJECT DISCUSSIONS.

We report here the original contribution made to this technical note by Keith Raney on 26 June 2008. This text was included within the main body of the Technical Note, distributed across various sections, following request by ESA at the SAMOSA Progress Meeting #3 (Starlab, 19 June 2008). However, the same text is reported here in its entirety to preserve the context and self-consistency of these comments.

**Suggested for the opening section of WP2 TN (See Section 2)**

A major objective is to verify the improvement in sea surface height (SSH) measurement precision as a function of significant wave height (SWH) that has been predicted in theory as a benefit of a SAR mode radar altimeter. This verification was planned to be based on the analysis of actual data (such as should be available from CryoSat), and/or simulated data (as is available from the CRYMPS CryoSat simulator). This objective has not yet been achieved, but as summarized in this technical note, sufficient progress has been made such that strategies have been identified that when implemented will meet that objective.

Since CryoSat data will not be available in the near future, the initial verification exercises must rely on CRYMPS data. That implies that simulated data corresponding to the SAR mode and the LRM mode have to be compared quantitatively, for observations of the same input sea-state conditions. The simplest way to generate the required data is to run CRYMPS once over a given sea-state scenario, and to generate simultaneously two sets output waveforms, one corresponding to a SAR mode data set, and the other corresponding to an LRM mode data set. (In the event that the “one run-two output” strategy is not feasible, equivalent data pairs could be obtained from two separate (SAR-mode and LRM-mode) CRYMPS runs over identical input scenarios.) This technical note describes necessary steps to qualify CRYMPS data for quantitative mode comparisons, and offers recommendations for implementing said comparisons.

**Implied requirement: a “control experiment” on CRYMPS data (see Section 10)**

As detailed in WP2 TN, the sea surface sampling schemes for the two modes differ significantly. Thus, it has proven to be not straightforward to generate reasonable pseudo-LRM mode data from the (simulated) SAR mode data. The results from RDSAR Version 1 and Version 3 have raised as many questions as answers. The report summarizes several of the detailed issues that remain unresolved, including specific aspects of tracking and internal waveform consistency that are not revisited here.

Of more general interest is the lingering question whether CRYMPS data are up to the task of supporting quantitative mode-to-mode comparisons, based on transforming SAR-mode data to pseudo-LRM mode data. Two logical experiment classes are required to address this issue: (1) qualification of CRYMPS data (the “control” experiment”, and (2) quantified comparison of the measurement precision of the two modes (the “verification” experiment). In other words, before verification, the basic suitability of CRYMPS data products for comparisons must be established. One approach to the required control experiment for CRYMPS data is outlined in the Recommendations section of this

Technical Note. Once CRYMPS data are so qualified, then there are robust options for moving ahead with the intended comparison of the two modes. Again, one approach is outlined in the Recommendations section.

Given the logical equivalence between the simulated and the actual SAR mode data, the value of a verified methodology of generating pseudo-LRM data from the SAR mode takes on added importance. Once an algorithm and methodology is verified with simulated data, then the same approach could be applied to CryoSat data, over a wide variety of oceanic or inland water conditions. The results should have considerable value beyond the lifetime of the SAMOSA project itself.

**Comments on specific algorithms (see Section 10)**

Several high-level "lessons learned" follow from the investigations reported in this technical note:

**On pre-summing**. The initial approach (Version 1), which was motivated by an effort to conserve (additive) SNR, led to peaked waveforms quite unlike the intended LRM Brown-model waveforms. This peakedness is a consequence of the pulse-to-pulse correlation produced by the pulse-limited area on the (simulated) surface. As such, it provides an indirect confirmation of the fidelity of the CRYMPS simulation of the details of oceanic backscatter. However, the lesson learned is that the SAR-mode-to-pseudo-LRM transformation algorithm should not use presuming, or any form of coherent pulse-to-pulse combination for that matter. That conclusion is implicit in the upper bound on radar pulse-repetition frequency (PRF), the incoherent limit described by Walsh (1982).

**Doppler selection**. An alternative to pre-summing is to take the Fourier transform of the data in azimuth, across the data at a constant range over each burst, in the same way that opens the delay-Doppler algorithm. This would redistribute the samples by Doppler bin, which correspond to spacing at the surface of about 250 meters. Since the resulting waveforms reside in disjoint (Doppler) frequency bands, they would be statistically independent. However, one consequence of Doppler binning is to change the shape of the resolved backscatter area to be Doppler delimited along track and pulse-limited across track. The result? A peaked waveform, in this instance because of the asymmetrical footprint, rather than pulse-to-pulse correlation. Hence, along-track Doppler decomposition must be avoided in this context. Of course, an along-track FFT when viewed in the abstract is a form of "coherent summing", and so should be ruled out by application of the principle above.

**Waveform selection**. Within a given SAR-mode burst, the PRF is higher than that of the LRM mode by approximately a factor of 9. Thus, consider a sub-set of pulses comprised of every ninth pulse within a SAR-mode burst. The resulting waveforms approximate closely their counterparts in the LRM mode, especially with respect to pulse-to-pulse correlation. The general lesson learned here is that taken individually, none of the waveforms "know" that they are part of a SAR-mode sequence, as opposed to an LRM sequence. It follows that a subset of waveforms so selected from a SAR-mode burst (at least for that subset) represent the closest possible imitation of LRM mode data that the SAR-mode data conveys.

**Statistics and degrees-of-freedom**. Given that waveforms are selected carefully within the confines of each burst, and at a rate comparable to the LRM PRF, between bursts there are no waveforms available from the SAR mode. This is in contrast to the LRM mode, in which waveforms occur regularly regardless of where the SAR bursts may be. Measurement statistics in general—and variance in particular—depend intimately on the number of independent waveforms that are averaged (incoherently summed). Thus, if the two modes are to be compared based on SAR-mode-derived waveforms, then the discrepancy in the number of independent waveforms has to be accounted for. A method that respects this constraint is described in the recommendations.

**Contributions to Recommendations (see Section 11)**

**On time of observation**. As is well known, measurement variance is reduced as the degrees-of-freedom in the measurement is increased. Thus, if the objective is to establish the relative difference in measurement precision between modes, then the basis for comparison must span as large a number of pulses as is reasonably possible, rather than being confined to a short basis, such as 1/20 of one second. Second, as long as the underlying surface features are (statistically) invariant, then it does not matter how long the (simulated) observation lasts. Thus, to increase the confidence in any estimate of the difference in measurement variance between the two modes, then the averaging time should be as long as possible. At the outset, this will be limited by the length of CRYMPS runs (less potential end effects, if any). As a corollary, the primary comparison should be based on measurement precision, and the statistics of shorter averaging times, or of the mode's response to a change in sea-state, should take second priority.

**CRYMPS qualification**: the control experiment. Regardless of the algorithm employed to derive pseudo-LRM waveforms from SAR-mode waveforms, there must be a test to verify that the method is reliable. In principle, the candidate algorithm should be applied to SAR-mode data for a given input scenario, for which there also exist LRM waveforms. Then the test is comprised of quantitative comparisons of the pseudo-LRM measurements with the LRM measurements. These tests must demonstrate statistical equivalence. Any SAR-mode-to-pseudo-LRM mode transformation algorithm must pass this test before the pseudo-LRM data that it generates can be qualified for use in further experiments and comparisons.

A simple method to generate pseudo-LRM data is comprised of four steps: (1) run CRYMPS once over a constant sea-state scenario (to generate simultaneous SAR mode and LRM mode waveforms); (2) choose n seconds of contiguous LRM waveforms, resulting in a group of nxPRFLRM waveforms; (3) select nxPRFLRM waveforms from the SAR-mode bursts (noting that this will require a sequence of SAR-mode data nearly 3 times longer in order to gather exactly the same number of waveforms as in the LRM group); and (4) compare the statistics of the two groups. Such a control experiment gets data in the "true-LRM" mode and from the "pseudo-LRM" mode that should be statistically identical. The averaging time should be as large as possible in order to expose small differences in the variances of the results.

For example, if the intended interval is one second (n=1), then the LRM mode data would have 1970 waveforms. The pseudo-LRM data would require the underlying SAR mode sequence to last nearly three seconds to supply an equal number of waveforms. Eight waveforms should be selected from each SAR-mode burst, one waveform of every 9. This should be repeated for about 250 bursts, to accumulate 1970 waveforms. The essential points are (i) that the same number of waveforms be assembled for both modes, and (ii) during a burst interval that the same PRF be replicated (as closely as the burst mode allows). In principle, the two sets of waveforms (square-law detected and compressed) from the LRM run and the SAR-mode run should be statistically identical. If this proves to be true, then CRYMPS SAR-mode individual waveforms can be accepted with confidence to be the statistical equivalent to individual waveforms from the LRM mode. If not true, then CRYMPS would have to be enhanced to pass this or any similar test before its data could be used as intended for WP2. (Note: Variations on this validation experiment include proportionally reducing the length of the two runs if required, and running the same procedure over two or more SWH scenarios.)

**Quantitative comparison of modes:** the validation experiment. Once confidence is established in the transformation of SAR-mode data into pseudo-LRM data that is statistically equivalent to “true” LRM data, then SAR-mode data (either from CRYMPS or CryoSat) are sufficient to set up experiments to investigate the relative performance of the two modes under a variety of sea-state conditions. The method is loosely patterned after the design of the control experiment. To summarize, a validation experiment is comprised of three steps: (1) select individual waveforms from SAR-mode data (as described above) of duration approximately three times as long as the intended averaging time n seconds to assemble the pseudo-LRM group; (2) select the corresponding SAR-mode data of duration n seconds; (3) calculate the desired statistics on the two groups each representing n seconds of observation in their respective modes, and compare. Note that the basis for comparison must be the same equivalent observation (averaging) time n seconds for both, since that is the only fair way to compare their performance. Of course, it takes a longer time to assemble the pseudo-LRM data group, but that is irrelevant to the comparison, which must be faithful to the statistics, especially regarding the “degrees-of-freedom” of the two types of measurement, per unit time.

**Trade-offs**. Since the SAR mode and the LRM mode PRF patterns are so different, some compromise in the experiment boundary conditions has to be accepted before the resulting “true” and “pseudo” LRM waveforms can be expected to converge to statistical similarity. Candidate parameters for trade include, for example, adjusting the variances to account for any difference in the number of independent waveforms summed in each case, or crafting “filler waveforms” to stand in for the missing ones. Other compromises include the strategy outlined above, namely, the use of pseudo-LRM waveforms selected from a longer duration of the SAR-mode data so that when the two modes are compared statistically, they correspond to the correct number of pulses in each case that would be observed in a given time interval. All such schemes imply advantages as well as disadvantages. The trade-off should favor the most reliable result with the least affront to the underlying physics. The method outlined above is recommended, based in part on the experience gained to date on SAMOSA.

**Waveform posting rate.** The project should give serious consideration to expanding the nominal period of comparison from 1/20 second to as long as the simulation can support. Given that the objective is to compare the intrinsic precision of two different radar altimeter architectures, rate of waveform posting is irrelevant. If shorter posting intervals are of interest, then the resulting variances of a longer observation time can be scaled (by the square root of the time ratio) to a shorter time. Scaling to shorter time intervals from long is far more robust than attempting to scale short-time variances to long-term measurements.

**Observation times.** There is no fundamental requirement that the data collection time for the waveforms required to assemble the pseudo-LRM data must equal the intended averaging time for the end comparisons. Indeed, this degree of freedom is the least risky of those that one might consider when trying to bring the statistics of the two modes into convergence. Set up the input scenarios so that the dwell time in each sea state is sufficiently long that the SAR-mode data will have enough time to accumulate an equivalent number of statistically independent waveforms in the pseudo-LRM mode as an equivalent LRM mode. It is worth noting that this method should apply equally well to actual CryoSat data.

**Waveform accommodation**. SAR-mode waveforms are peaked, in contrast to the conventional “Brown-model” LRM waveforms. Comparison between these two types requires compatible retracking and parameter estimation algorithms. Jensen (J. R. Jensen, "Radar altimeter gate tracking: theory and extension," IEEE Transactions Geoscience and Remote Sensing, vol. 37, pp. 651-658, 1999) derived an algorithm that transforms SAR-mode (delay-Doppler) waveforms into conventional waveforms. The project should consider adopting the Jensen transformation (or an equivalent operator) so that the measurement precision ascribed to data from the two modes may be compared reliably.